

AD/A-006 663

NEW RAY OPTICS MODEL FOR THE
DIRECTIONAL DISTRIBUTION OF LIGHT
REFLECTED FROM A ROUGH SURFACE

T. S. Trowbridge, et al

Naval Missile Center
Point Mugu, California

25 February 1975

DISTRIBUTED BY:

NTIS

National Technical Information Service
U. S. DEPARTMENT OF COMMERCE

UNCLASSIFIED

SECURITY CLASSIFICATION OF THIS PAGE (When Data Entered)

REPORT DOCUMENTATION PAGE		READ INSTRUCTIONS BEFORE COMPLETING FORM
1. REPORT NUMBER TP-75-01	2. GOVT ACCESSION NO.	3. RECIPIENT'S CATALOG NUMBER AD/A-006663
4. TITLE (and Subtitle) NEW RAY OPTICS MODEL FOR THE DIRECTIONAL DISTRIBUTION OF LIGHT REFLECTED FROM A ROUGH SURFACE		5. TYPE OF REPORT & PERIOD COVERED
7. AUTHOR(s) T. S. Trowbridge and K. P. Reitz		6. PERFORMING ORG. REPORT NUMBER
9. PERFORMING ORGANIZATION NAME AND ADDRESS Naval Missile Center Point Mugu, California 93042		8. CONTRACT OR GRANT NUMBER(s)
11. CONTROLLING OFFICE NAME AND ADDRESS Naval Air Systems Command Washington, DC 20360		10. PROGRAM ELEMENT, PROJECT, TASK AREA & WORK UNIT NUMBERS AIRTASKs A30303/225/70F20- 311-003 and A36533/225/ 70F20-344-601
14. MONITORING AGENCY NAME & ADDRESS (if different from Controlling Office)		12. REPORT DATE 25 February 1975
		13. NUMBER OF PAGES 39
		15. SECURITY CLASS. (of this report) UNCLASSIFIED
		15a. DECLASSIFICATION DOWNGRADING SCHEDULE
16. DISTRIBUTION STATEMENT (of this Report) Approved for public release; distribution unlimited.		
17. DISTRIBUTION STATEMENT (of the abstract entered in Block 20, if different from Report)		
18. SUPPLEMENTARY NOTES PRICES SUBJECT TO CHANGE		
19. KEY WORDS (Continue on reverse side if necessary and identify by block number) Geometrical optics Polarization Target designation Laser Reflection Light Rough surface		
20. ABSTRACT (Continue on reverse side if necessary and identify by block number) A new ray optics model is presented for the reflection of light (both within and without the nominal plane of incidence) from the rough air/material interface of a randomly rough surface. Such reflection is of particular interest to laser target designation systems. Unlike previous derivations that modeled the rough interface as consisting of microareas randomly oriented but flat (facets), this derivation models it as consisting of microareas not only randomly oriented but also randomly curved. Physically, the models are the same, but this new derivation leads to some new and useful (continued)		

DD FORM 1 JAN 73 1473 EDITION OF 1 NOV 65 IS OBSOLETE

UNCLASSIFIED

SECURITY CLASSIFICATION OF THIS PAGE (When Data Entered)

Reproduced by
**NATIONAL TECHNICAL
 INFORMATION SERVICE**
 US Department of Commerce
 Springfield, VA. 22151

UNCLASSIFIED

SECURITY CLASSIFICATION OF THIS PAGE(When Data Entered)

20. ABSTRACT (Concluded)

results: (1) It is found that, for any given rough interface, there exists a single optically smooth curved surface of revolution ("average" irregularity) of very restricted shape that will reflect light in the same distribution as that reflected by the rough interface. (2) Modeling this "average" irregularity as an ellipsoid of revolution gives a surface structure function that is more accurate and useful than previously existing ones. (3) Unlike the "facet" derivations, this derivation lends itself to a normalization giving the absolute reflectance-distribution function. Reflection by this new interface model, combined with some Lambertian reflection, is tested extensively both within and without the nominal plane of incidence on a variety of rough surfaces and is found to apply rather well.

UNCLASSIFIED

1 a SECURITY CLASSIFICATION OF THIS PAGE(When Data Entered)

NAVAL MISSILE CENTER

AN ACTIVITY OF THE NAVAL AIR SYSTEMS COMMAND

IRA N. SCHWARZ, CAPT USN
Commanding Officer

THAD PERRY
Technical Director

This report describes work accomplished under AIRTASKs A30303/225/70F20-311-003, Air Weapon Systems Investigations, and A36533/225/70F20-344-601, Surface Target Guidance (Missile Guidance Applications).

ACCESSION for	
NTIS	Write Section <input checked="" type="checkbox"/>
DDO	Ref Section <input type="checkbox"/>
WPA: C-1000	<input type="checkbox"/>
JUSTIFICATION	
BY	
DISTRIBUTION/AVAILABILITY CODES	
WPA: C-1000	
A	

Technical Publication TP-75-01

Published by Editing and Writing Branch
Technical Publications Division
Photo/Graphics Department
Security classification UNCLASSIFIED
First printing 140 copies

14

ACKNOWLEDGMENTS

The authors are indebted to C. T. Luke and C. A. Oleson for designing and supervising the measurements; to G. B. Matthews and A. Akkerman, colleagues in executing the measurements; C. A. Kent for consultation, and F. E. Nicodemus of the Naval Weapons Center for aid in terminology and other constructive criticism.

CONTENTS

	Page
SUMMARY	1
NOMENCLATURE	3
INTRODUCTION	4
Lambert's Law	4
Lommel-Seeliger Law	5
High- and Low-Reflectance Surfaces	5
Bouguer Facet Theory	5
Other Mechanisms	6
Diffraction Mechanisms	6
Rigorous Solutions of Maxwell's Equations	7
A Generalization	7
New Model for Ray-Theory Reflection	7
Organization of Report	8
INTERFACE REFLECTION MODEL	8
Reflection From a Single Microarea	8
Ensemble of Microareas and the Surface-Structure Function	11
Average Surface Irregularity	14
Model in Terms of Measurable Variables	17
Microarea Reflection Coefficient	18
Normalization	21
Ellipsoid of Revolution Average Surface Irregularity Approximation	22
COMPARISON TO MEASUREMENTS	23
CONCLUSIONS	29
REFERENCES	30
APPENDIX	
Proof that x is Finite When the Slope of $h(x)$ is Vertical	33

Preceding page blank

CONTENTS (Concluded)

	Page
TABLE	
1. Optimum Values of the Model Parameters	25
FIGURES	
1. Reflection From a Curved Microarea of the Rough-Surface Air/Material Interface	9
2. Specification of the Shape of a Curve Microarea in Terms of Two Orthogonal Curved Lines	11
3. The Concept of an "Average" Surface Irregularity	15
4. Relation Between the Local and Macrosurface Planes of Incidence	20
5. Comparison of Best Fits of Some Surface-Structure Functions (Equivalent to the Microarea or Facet Distribution Function)	24
6. Comparison of Some Theoretical and Measured Values of BRIDF for a Variety of Flat Rough Surfaces	26

TP-75-01
25 February 1975

NAVAL MISSILE CENTER
Point Mugu, California

**NEW RAY OPTICS MODEL FOR THE DIRECTIONAL
DISTRIBUTION OF LIGHT REFLECTED FROM A
ROUGH SURFACE**

(AIRTASKS A30303/225/70F20-311-003
AND
A36533/225/70F20-344-601)

By
T. S. TROWBRIDGE and K. P. REITZ

SUMMARY

This report presents a new model for ray-optical reflection from the rough, air/material interface of a randomly rough surface. We review the current understanding of light reflection from rough surfaces and show how the unique features of this new model contribute.

The new model, instead of treating the rough, air/material interface as being composed of randomly oriented flat microareas (facets), treats the interface as an ensemble of randomly oriented, randomly curved microareas. These two models are identical (physically) and are found to give the same results. However, this new derivation leads to some new and useful results. (1) A new visualization of the surface structure (an "average" irregularity) is conceived and proved valid. An average irregularity is an optically smooth curved surface of revolution of a shape such that it gives the same distribution of reflected light (when irradiated by a uniform, well-collimated beam) as that given by the actual rough-surface microstructure (when irradiated by the actual, nonuniform, well-collimated beam). (2) It is found that the shape of this surface of revolution may be greatly restricted and still be general enough to represent any physically realistic microstructure. (3) Modeling this average irregularity as an ellipsoid of revolution gives a surface structure function that is more accurate and useful than previously existing ones. (4) Unlike the "facet" derivations, this derivation lends itself to a normalization giving the absolute, instead of just the relative, reflectance-distribution function.

Reflection by this new interface model, combined with some Lambertian reflection, is tested extensively both within and without the nominal plane of incidence on a variety of commonly occurring rough surfaces. This, we believe, is the first time a theory of ray reflection from the interface is extensively tested outside the nominal plane of incidence. Such reflection is of particular interest to laser target designation systems. Data for 3M Black Velvet paint, soiled olive drab paint, cement, plywood, and grass, were used, and the parameters of the model were optimized to give the best fit of the model to the data. The comparisons were in general reasonably good (rms deviations of 20 to 35 percent), and the discrepancies could be mostly explained by the existence of gross deviations of some of the measured surfaces from the assumed surface, such as the existence of two surface materials instead of just one and the existence of a significant directional dependence of the surface structure. Also, the normalization was verified in a rough manner.

Publication UNCLASSIFIED.

NOMENCLATURE

Symbol	Definition
\hat{l}	Unit vector pointing in the direction from which the light is incident.
\hat{r}	Unit vector pointing in the direction of reflection.
\hat{n}	Unit vector pointing in the direction of the microsurface normal.
β	Zenith angle of incidence, relative to the macrosurface.
θ, ψ	Elevation and azimuth angles of reflection, relative to the macrosurface.
α, α'	Zenith and azimuth angle of the microsurface normal, relative to the macrosurface.
s	Zenith angle of incidence relative to the microsurface.
ϕ	Angle between the microscopic and macroscopic planes of incidence.
γ	Angle between the incident polarization plane and the macroscopic plane of incidence.
n, k	Indices of refraction and absorption of the surface material.
$\delta(s)$	Fresnel reflection coefficient of the surface material (any subscript indicates the polarization state of the incident light).
ΔA_i	A small area on the microsurface.
$D(a)$	The surface structure function, or the relative amount of microsurface area oriented in a given direction.
e	Ratio of the axis revolved about to the axis revolved for the ellipsoid of revolution average surface-irregularity.
$\rho_s(a)$	Radius of curvature of the surface of revolution average surface-irregularity in the plane through the rotation axis.
$\rho_s(s)$	Radius of curvature of the surface of revolution average surface-irregularity in a plane perpendicular to the rotation axis.
f_{rl}	BRPDF or bidirectional reflected-radiance-distribution function. The ratio of the radiance reflected (into a chosen direction) to the irradiance incident in a collimated beam (from a chosen direction).
f_{ri}	BRIDE or bidirectional reflected-intensity-distribution function. The ratio of the radiant intensity [W/sr^{-1}] reflected (into a chosen direction) to the radiant power [W] incident (from a chosen direction). $BRPDF = BRIDE \sin \theta$. For a Lambertian surface, $BRPDF = \text{Const. occurs.}$
f_{rls}	Component of the BRIDE contributed by reflection from the rough air/material interface.

Preceding page blank

Symbol	Definition
f_{rLL}	Lambertian component of the BRIDF.
ρ_L	Lambertian component of the directional-hemispherical reflectance, which is the ratio of the total radiant power [W] reflected into all directions to the radiant power incident [W] (from a chosen direction).
σ_m	The minimum value found during optimization for σ , the rms of the difference between the theoretical and experimental values of the BRIDF divided by the theoretical value.

INTRODUCTION

In this report, we wish to present some contributions to the understanding of the reflection of light from rough surfaces.* For simplicity, we consider only rough surfaces that are flat on a macroscopic level but rough on a microscopic level. The microscopic irregularities are assumed to have random shape and distribution over the surface and no preferred orientation in any direction along the plane of the macrosurface (a uniform, symmetric, rough surface). For perspective, the following brief summary of the current understanding of light reflection from such surfaces is presented.

Lambert's Law

The first theory of light scattering by a rough surface, Lambert's Law, can be derived by considering the incident light ray to be "completely randomized" by the rough surface. By completely randomized is meant a purely hypothetical situation in which an incident ray emerges from the surface (unaffected by the air-material interface) after last being scattered isotropically and with equal likelihood from every point in the semifinite space below the surface plane. Lambert's Law states that the reflected radiance (reference 1) [$\text{W sr}^{-1} (\text{proj. cm}^2)^{-1}$] (or the familiar property of visual brightness) is invariant with observation direction, and, for constant incident irradiance, [W cm^{-2}] is invariant with incidence direction.** Also, Lambert's Law states that the reflected light is unpolarized and independent of incident polarization. However, many surfaces do not even vaguely follow Lambert's Law. The best diffusing surfaces known deviate a few percent (references 2 and 3) even at zero zenith angles of incidence and reflection, and differ grossly at zenith angles greater than 45 degrees. There are two mechanisms that tend to randomize the incident light and thus tend to produce Lambertian reflection: multiple reflection from the irregularities of the rough, air/material interface and multiple scattering from inhomogeneities within the material below the interface. The multiple reflection mechanism is considered secondary, since it is found (reference 4) to contribute only a few percent to the reflection from most dielectric surfaces. Most of this reflection may be from only double reflection and thus not randomized completely.

*This work was supported by the Naval Air Systems Command under AIRTASKs A30303-225-70F 20-311-003 Air Weapons System Investigations, and A36533/225/70F 20-744-601, Surface Target Guidance (Missile Guidance Applications).

**As an aid to the reader, the units of each term or quantity will follow it in brackets. Area units preceded by "proj." refer to the area of a surface projected onto a plane perpendicular to the propagation direction of the light. Other area units refer to an area upon a surface.

The multiple scattering is the primary mechanism for randomizing the incident light and acts as follows. Light entering the surface material is somewhat randomly scattered by refraction at the rough, air/material interface. Then the light is randomly scattered one or more times by inhomogeneities within the material. Finally, it is again somewhat randomly scattered by refraction upon exiting the interface. (A similar mechanism has been evaluated numerically in reference 5.) Thus, three or more random scatterings must occur, and three should greatly randomize the light. However, light is completely randomized only after an infinite number of random scatterings; thus, some non-Lambertian light could emerge. Also, it has been shown (reference 6) that the light becomes partially polarized (in contradiction to Lambert's Law) upon exiting the rough, air/material interface and that such polarization can be quite pronounced at large zenith angles of reflection. Thus the light can be partially de-randomized upon exiting the interface.

Lommel-Seeliger Law

The above described multiple-scattering can be divided into scattering at the interface and scattering below the surface. The below-surface scattering should contribute the most to the randomization of the multiple-scattered light. Below-surface scattering has been treated extensively (see references 7, 8, and 9 for summaries). The Lommel-Seeliger Law was derived by considering only single, isotropic scattering by below-surface scatterers and below-surface attenuation before and after scattering. Even though light reflected in this way is not at all randomized, it was found to give only a slight deviation from Lambert's Law. The Lommel-Seeliger Law was extended by including nonisotropic scattering (various "phase functions" for the scatterers) and double scattering. Chandrasekhar (reference 10) succeeded in including all orders of multiple scattering below the surface. His results for some phase functions, especially the isotropic, did not deviate much from Lambert's Law except at large zenith angles of incidence and reflection.

Shadowing of parts of a Lambertian surface by the surface irregularities was also considered (references 7 and 11). Such shadowing tends to produce a peak reflection in the direction of the source, but is not usually a large effect.

Thus the above mechanisms may not produce perfectly Lambertian reflection, but the imperfections cited cannot fully account for the large deviations from Lambert's Law found for many surfaces.

High- and Low-Reflectance Surfaces

Dark, or low-reflectance, dielectric surfaces are found to deviate the most from Lambert's Law. For dielectrics, the reflection from the air/material interface is low (a few percent) and varies little for various materials. The rest of the incident light (~95 percent) passes into the surface material, where it, and thus the reflectance, is strongly affected by the absorption coefficient, which varies greatly with the material. If the coefficient is high, the below-surface reflectance can be zero, leaving only the interface reflectance, which is always low. Thus, for low-reflectance surfaces, reflection from the interface is much more significant. Also, this reflection is found (reference 4) to be almost entirely single reflection, which is not at all randomized and thus might deviate grossly from Lambert's Law.

Bouguer Facet Theory

A theory for single reflection by a rough, air/material interface was first presented by Bouguer (reference 12) about 1760. The interface is modeled as consisting of randomly oriented, optically flat facets, each of which behaves like a small plane mirror, reflecting a portion of the light incident on it as determined by Fresnel's equations for specular reflection at a flat dielectric interface. For collimated incident light, those facets of only one orientation can reflect light into a given direction. Thus, all light in that direction has been reflected in exactly the same way, so it is not at all randomized, and the reflection by the facet mechanism is not at all Lambertian.

The Bouguer facet theory has been found to explain much of the non-Lambertian reflectance and has undergone considerable development. (1) The derivation of the basic theory has been refined (references 13 through 19). (2) Several models (references 13, 17, 18, and 20 through 22) have been tried for the "microarea distribution function." This is the function that gives the relative number of facets oriented in any given direction, or, more precisely, the relative total facet surface area per unit solid angle of surface normals pointed in any given direction. This function governs the directional distribution of the scattered light. If the function is uniform with respect to the direction of the facet normals, a diffuse-like distribution occurs. If most of the facets lie nearly parallel to the plane of the surface, a nearly specular distribution occurs. (3) Another development of the facet theory is the inclusion of shadowing (references 11, 14, 17, 19, and 23); that is, some facets cannot contribute to the reflection because they are in the shadow of neighboring irregularities. The shadowing theory results in a "geometrical attenuation factor," the reflection in any direction being reduced by a complicated function of only the direction of incidence and reflection. Shadowing has been found (reference 19) to be the only mechanism able to explain the sharp cutoff of light near grazing reflection. (4) Another and recent development is the extension of facet theory (reference 19) to cover reflection outside the plane of incidence. However, there has been little comparison with measurements outside of the plane of incidence.

Other Mechanisms

There are some other mechanisms possibly contributing to rough-surface reflection. There may be randomly oriented facet-like areas, "rough facets," each of which reflects as a little flat Lambertian reflector (reference 16), resulting on more light being scattered at higher zenith angles of reflection than from the ideal large flat Lambertian surface. This might be the case if the below-surface scattering originated mostly from a depth that was much smaller than the typical size of the facets.

There may be reflection from a planar lower boundary to the rough-surface material, as, for example, for painted flat surfaces. This is found (reference 24) to explain some reflection phenomena.

There may be Bouguer-like facet reflection from below-surface cracks. This type of reflection produces effects differing from those of surface-facet reflection and helps to explain some phenomena (reference 25).

Diffraction Mechanisms

The Bouguer mechanism and the above mechanisms are based on ray optics and thus require that the size of the surface irregularities and all their radii of curvature be much greater than the wavelength of the light (references 26 and 27). This, of course, may not always be true, so some of the reflection may be explainable only by wave optics. Beckmann and Spizzichino (reference 28) give the basic theory of the application of diffraction theory to reflection from the rough interface of a randomly rough surface. Many physically important results are obtained in closed form, but they are complex and limited, for example, infinite series often result, few polarization phenomena can be treated, and shadowing has to be ignored. One very significant result of the effects of wave optics is the Rayleigh Criterion (references 14 and 29). This criterion implies that at close enough angles to grazing incidence on a rough surface, which at all other angles of incidence reflects according to ray optics, there will appear a specular reflection caused by diffraction. The larger the irregularities and their radii of curvature, the smaller the required grazing angle will be, but the diffraction-caused specular reflection will ultimately appear. Relevant to ray reflection at the air/material interface, Beckmann obtains a closed form solution in the large irregularity limit for a surface characterized by a Gaussian distribution of surface heights and an autocorrelation length along the surface. Such a characterization merely implies another microarea distribution function.

On most real surfaces, the microstructure probably includes some parts whose reflection can be approximated by ray optics and other parts whose reflection must be treated by physical optics. One would suspect that usually the broad facet-like areas, being large and flat, could be treated by ray optics, but that the corners and edges of these areas, being small and highly curved, must be treated by physical optics. Much recent work (references 30 through 37) has been done on diffraction from edges and corners, resulting in some simple expressions for the reflected light distribution and some ways for experimentally separating the diffracted light from the ray-reflected light. The diffraction-scattered light was predicted to be quite specular.

Rigorous Solutions of Maxwell's Equations

When the wavelength becomes large enough relative to the size of the scattering irregularity, diffraction formulae such as those of Beckmann and Spizzichino (reference 28), based as they are on a scalar wave equation, predict results that deviate significantly from the results obtained from a rigorous application of Maxwell's equations. This topic has been the subject of much effort (and some controversy) in the IEEE Journal of Antennae and Propagation during 1971, 1972, and 1973.

A Generalization

Although deviations in some directions and for many surfaces are large, it appears (references 14, 17, 20, 38, and 39) that most of the reflection in most directions for most rough surfaces is closely approximated by a combination of Lambertian reflection from below the interface and simple (no shadowing) Bouguer reflection from interface facets. This is reasonable theoretically because: diffraction phenomena are generally limited to a narrow region near the specular direction; shadowing produces extremely large effects only near low elevation angles of reflection; multiple-surface scattering is found to be small; below-surface particle scattering tends to be nearly Lambertian; reflection from a below-surface plane should usually be small because of attenuation in the surface material; mirror reflections from below-surface facets will be somewhat randomized from entering and exiting the rough, air/material interface; and the "rough-facet" reflection cannot give really radical departures from Lambertian reflection.

New Model for Ray-Theory Reflection

This report presents a new model for ray-theory reflection from the rough, air/material interface. Instead of randomly oriented flat microareas (facets), the surface structure is here modeled as an ensemble of randomly oriented, randomly curved microareas. Since for practical purposes any curved area can be broken down into infinitesimal facets, the two models are identical (physically) and thus must give the same results. However, this new derivation leads to some new and useful results; that is, a new visualization of the surface structure (an "average" irregularity) is conceived and proved valid; a new, more accurate, and useful function representing the surface structure is discovered (resulting from an ellipsoid of revolution as the "average" irregularity); and a way to normalize the resulting reflection equations to give the absolute, instead of just the relative, reflectance distribution is found.

This model is then combined with some Lambertian reflection and tested on data from a particular application of interest. The application of interest is to laser target designation systems. A laser illuminates a point on a target and a receiver, on a piece of ordnance or on a fire control system, detects the direction of the illuminated point and directs the ordnance. The geometry for this application consists of incidence from any angle of a polarized collimated beam onto a flat rough surface; observation from a distance such that the illuminated area is, for practical purposes, a point; and observation of the reflected light from any direction, both within and without the plane of incidence (we believe that

this is the first time a theory of ray reflection from the interface is extensively tested outside the plane of incidence). The model is limited to simply a combination of ray reflection from the rough, air/material interface and Lambertian reflection because this combination has been found (references 14, 17, 20, 38, and 39) to give most of the reflection in most directions from most surfaces, and because, for the application to target designation systems, a model is needed that gives only reasonable accuracy for a wide variety of common rough surfaces and uses as few surface-related parameters as possible. The comparison to the data was good. Discrepancies can generally be explained by gross deviations of some of the measured surfaces from the assumed surface, such as the existence of two surface materials instead of just one, and the existence of a significant directional dependence of the surface structure. The validity of the normalization is verified, and the usefulness of the concept of an ellipsoid of revolution as the average surface irregularity is demonstrated.

Because of the geometry described above, the usual and most generally useful quantity for expressing the reflectance distribution is poorly applicable, so a less generally used but more applicable quantity is adopted. Nicodemus (reference 40) calls the unusual quantity the BRRDF, r_{rL} , [$\text{W sr}^{-1}(\text{proj. cm}^2)^{-1}/\text{W cm}^{-2}$] (bidirectional reflected-radiance-distribution function), or for short, the BRDF, r_r (bidirectional reflectance-distribution function). It is defined as the radiance [$\text{W sr}^{-1}(\text{proj. cm}^2)^{-1}$] reflected into a given direction per unit irradiance [W cm^{-2}] incident on the surface from another given direction. This quantity involves radiance, which is very useful because it has certain invariance properties (reference 41) upon transformation through optical systems and upon reflection from surface to surface. However, irradiance is a density of light incident on a surface, and for our geometry, a reflectance-distribution function containing such a density is not the most useful quantity. Much better for our purposes is the BRIDF, r_{rI} , (bidirectional reflected-intensity-distribution function) (reference 42). It is defined as the radiant intensity [W sr^{-1}] reflected into any specified direction from an illuminated "point" per unit radiant flux [W] in the incident beam. To find the more generally useful BRRDF (or BRDF), simply divide the BRIDF by the cosine of the zenith (or sine of the elevation) angle of reflection.

Organization of Report

This report is organized as follows. For the derivation of the interface reflectance model, first the reflection from a single curved microarea is derived, then an ensemble of microareas is formed, resulting in a reflectance-distribution function in terms of a surface structure function, and the concept of an "average" irregularity is presented and validated. The model is put in terms of the laboratory coordinates, and the Fresnel reflectance of the surface material is found. Next, a normalization procedure is implemented to make the reflectance-distribution function an absolute quantity, and an ellipsoid of revolution is used as a one-parameter model for the average irregularity. For the comparison to measurements, some Lambertian reflection is added, and the resulting four-parameter reflection model is applied to reflectance-distribution function measurements both within and without the nominal plane of incidence on a variety of rough surfaces.

INTERFACE REFLECTION MODEL

Reflection From a Single Microarea

Consider, as shown in figure 1, a very small curved area ΔA on an irregularity of the rough-surface microstructure. This area is chosen small enough that we can approximate the curvatures in all directions on it by sections of circles. (The curvatures of the circle sections may be different in different directions across the area.) Also, the area is chosen small enough that the angles spanned by these circle sections are very small. This smallness allows the specification of the orientation of ΔA by a single surface normal \hat{n} . The direction of \hat{n} is given (relative to the planar macrosurface) by a zenith angle α and an azimuth angle

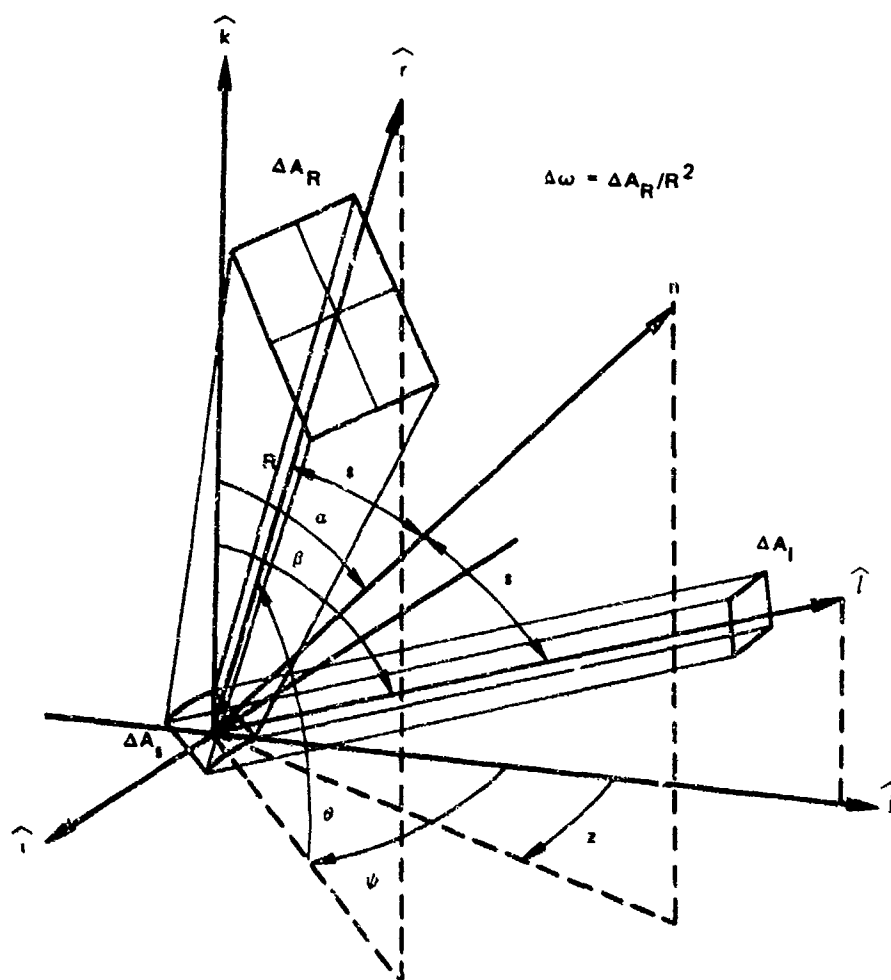


Figure 1. Reflection From a Curved Microarea of the Rough-Surface Air/Material Interface. A small, optically smooth, slightly curved area ΔA_s with a normal \hat{n} intercepts the light from an area ΔA_i of the incident beam and diverges it into $\Delta\omega$ steradians in a direction \hat{r} such that $\hat{r} \times \hat{n} = \hat{n} \times \hat{l}$.

z defined as shown in figure 1. Let the incident light be a narrow collimated beam originating from a source in the direction \hat{l} , and let the incident light have a radiant flux (reference 1) of Φ_l [W] spread (not necessarily uniformly) over the beam's cross-sectional area A_l . At the point in A_l where ΔA_s is located, let the incident normal irradiance* (flux per unit area projected perpendicular to the beam) be E_n [W (proj. cm^2) $^{-1}$].

Let ΔA_s be optically smooth and let its minimum dimension and its minimum radius of curvature be much greater than the wavelength of the incident light. Then (references 26 and 27) ray theory applies, so

*Irradiance [W cm^{-2}] is the flux incident upon a unit area of a surface. In an unchanging incident beam, the irradiance varies with the orientation of the surface (angle of incidence) and is thus not a constant of the beam. "Normal irradiance" [W (proj. cm^2) $^{-1}$] is the irradiance upon a surface oriented normal to the incident beam and thus is a constant of beam.

ΔA_s reflects as a section of a curved mirror surface; that is, of the incident light intercepted by ΔA_s , a portion $R(s, n, k)$ (determined by the Fresnel equations; n and k are the refraction and absorption indices, respectively) is reflected into a small cone (represented for simplicity by the rectangular cross section cone in figure 1) of solid angle $\Delta\omega$ [sr] in a direction \hat{r} determined by the mirror reflection equation $\hat{r} \times \hat{n} = \hat{n} \times \hat{l}$.

The reflected light is not, strictly speaking, in the form of a cone. It would be in the form of a true cone if the curvature of ΔA_s did not vary with the direction on ΔA_s , since ΔA_s would then be a spherical mirror, and the reflected light would radiate from a definite point image (real or virtual depending on the sign of the curvature). The vertex of this cone would lie along the reflection direction at a distance, before or after ΔA_s , determined by the magnitude and sign of the curvature of ΔA_s . But since the curvature in general does vary with direction on ΔA_s , the image point is smeared. But the rays reflected from ΔA_s (or their backward extensions in the case of a virtual image) all pass through a football-shaped volume of space approximately bounded in one direction by two points and in the other directions by the circumference of an area whose size is directly related to the size of ΔA_s . The two bounding points are the image points for spherical mirrors of curvatures equal to the maximum and minimum curvatures found on ΔA_s . Thus, except for the realistically impossible circumstance of a perfectly zero maximum or minimum curvature, the dimensions of this volume are finite. Now, let the observer be at infinity. To him, this volume, the smeared image, is effectively a point, and thus the reflected light is effectively a true cone. Also, this condition makes the position of the image point irrelevant (for convenience, let the cone vertex lie on ΔA_s).

We can now quantify the light reflected from ΔA_s as a radiant intensity (radiant flux per steradian radiating from a point source), since the light reflected from ΔA_s originates effectively from a point. This reflected radiant intensity [W sr^{-1}] is derived from the curvatures of ΔA_s as follows. Of the incident beam cross sectional area, the area intercepted by ΔA_s is $\Delta A_s \cos s$ [cm^2], and thus ΔA_s reflects a radiant flux of $R(s) E_n \Delta A_s \cos s$ [W] into the small solid angle $\Delta\omega$ [sr], giving the reflected radiant intensity $I = R(s) E_n \Delta A_s \cos s / \Delta\omega$ [W sr^{-1}]. Letting ΔA_s be small enough that it subtends only a small angle in any direction allows the curved lines Δl_a and Δl_z (see figure 2) to be very nearly straight lines. Thus, the approximation $\Delta A_s = \Delta l_a \Delta l_z$ holds, where Δl_z is the line segment formed on ΔA_s by the intersection of ΔA_s with a plane parallel to the macrosurface and Δl_a is the line segment formed on ΔA_s by the intersection of ΔA_s with the plane containing the macrosurface normal \hat{k} and the ΔA_s -surface normal \hat{n} . Since these line segments are sections of circles, they can be given by $\Delta l_z = \sigma_z |\Delta z|$ and $\Delta l_a = \sigma_a |\Delta \alpha|$, where σ_z and σ_a (defined positive) are the radii of curvature of ΔA_s , and Δz and $\Delta \alpha$ are the arcs subtended by Δl_z and Δl_a , respectively. Strictly, σ_z is not a radius of curvature of ΔA_s because it is not perpendicular to ΔA_s , but this does not affect the derivation. The reflected solid angle can be given by $\Delta\omega = \cos \theta |\Delta\theta \Delta\psi|$ [sr]. Substituting the above three expressions into I gives

$$I = \frac{R(s, n, k) E_n \cos s}{\cos \theta} \left| \frac{\Delta \alpha \Delta z}{\Delta \theta \Delta \psi} \right| \sigma_a \sigma_z \quad [\text{W sr}^{-1}]. \quad (1)$$

Since α and z are functions of θ , ψ , and β , the quantity $|\Delta \alpha \Delta z / \Delta \theta \Delta \psi|$ can be given by the Jacobian determinant $J(\alpha, z; \theta, \psi)$ (in the limit as the incremental angles approach zero).

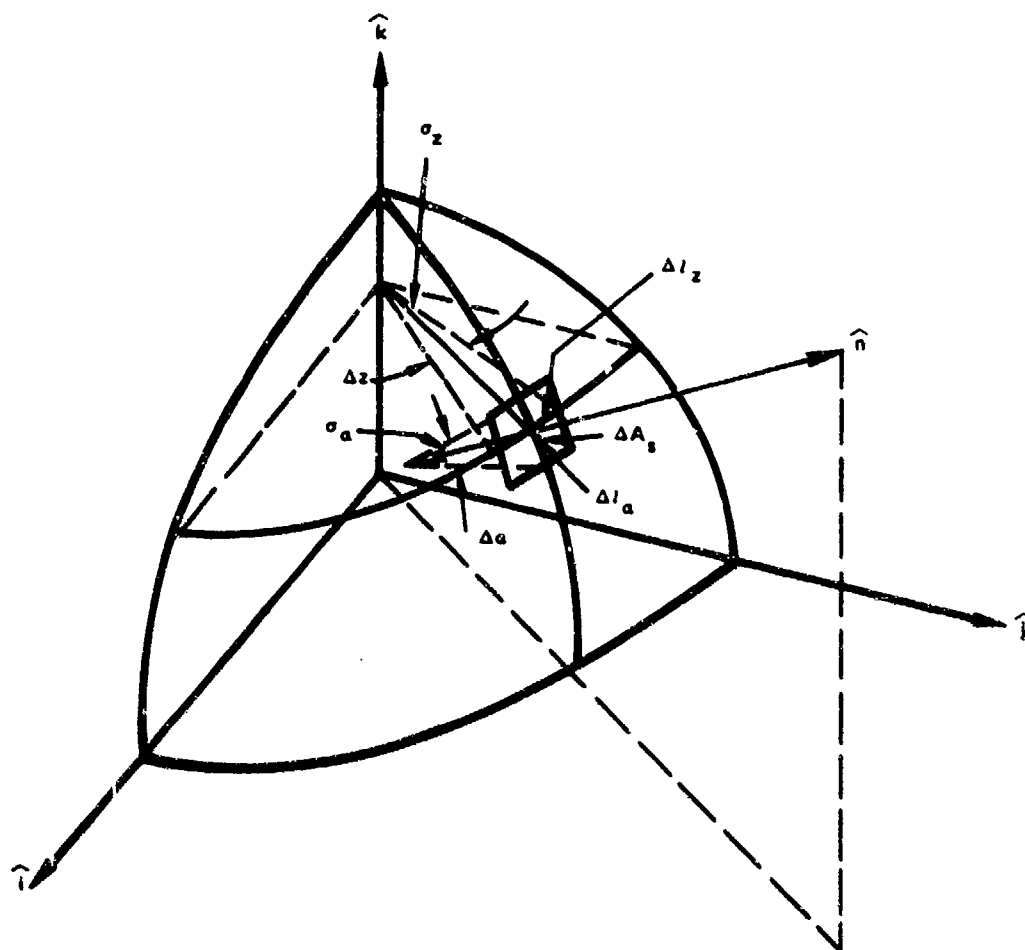


Figure 2. Specification of the Shape of a Curved Microarea in Terms of Two Orthogonal Curved Lines. A small, slightly curved element of surface area ΔA_s may be intersected by a plane parallel to the macro-surface to form the line Δl_z with a curvature radius of σ_z , and ΔA_s may be intersected by the plane parallel to \hat{n} and \hat{k} to form the line Δl_a with a curvature radius of σ_a .

Since α , z , s , and J are functions of only the laboratory coordinates (β , θ , and ψ), and n and k are parameters of only the surface material, the only quantities in equation (1) that depend on the size or shape of ΔA_s are σ_a and σ_z . Thus, the surface geometry appears in equation (1) only as the curvatures of ΔA_s . Also, the size of ΔA_s does not enter and may be disregarded.

Note that the derivation is still valid if either one or both of the lines Δl_z and Δl_a have a curvature opposite that shown in figure 2. This fact lets equation (1) apply to a curved area of any shape: convex, concave, or saddle. Also, since radii of curvature are defined as positive and the Jacobian determinant is used only in an absolute value, it remains unchanged if the curvatures of either Δl_a or Δl_z or both are reversed.

Ensemble of Microareas and the Surface-Structure Function

Consider the following model for the surface microstructure. Let the microsurface be continuously curved and randomly undulating, similar to hill or mountain topography. Let it be optically smooth and

let all curvature radii and irregularity sizes be much larger than the incident light wavelength. Let the ΔA_s be any small area on this undulating surface. Under these conditions, equation (1) gives the reflection from each small area. Equation (1) may be applied to a discontinuous microstructure if one disregards diffraction effects at corners and edges. This allows application of equation (1) to a randomly scratched surface, such as ground glass or roughened metal, and to a "globule pile"-like structure, such as some diffuse spray-painted surfaces. Also, equation (1) may be applied to a surface containing flat facets if one makes their curvature radii not quite infinite. A very wide variety of microstructures is thus included. Finally, let the statistical properties be uniform with position on the surface and independent of direction along the surface (no wood-like grain or scratches with a preferred direction).

For given directions of illumination and observation, an observer, if his visual resolution were sharp enough to resolve the surface microstructure, would see the reflected light originating only from various points scattered around the microstructure. These are points at which the microsurface normal happens to be in the proper direction for reflection to the observer. Since the illuminated macrosurface area is small and the receiver is at infinity, the relative locations of the reflecting points are irrelevant, and all the reflected light may be treated as if it originated from a single point. Thus we may speak of a reflected total radiant intensity I_T [W sr^{-1}] equal to the sum of the radiant intensities contributed by the individual reflecting points. Normals at the reflecting points must all be parallel, so the reflection I_i from each point is given by equation (1) with the same values of θ , ψ , α , z and s . If for a particular combination of incidence and reflection directions, a given incident beam illuminates N reflecting points, the total radiant intensity reflected in the specified direction is given by the ensemble

$$I_T = \sum_{i=1}^N I_i = \sum_{i=1}^N \frac{R(s, n, k) E_{ni} \cos s}{\cos \theta} \left| J \left(\frac{\alpha, z}{\theta, \psi} \right) \right| \sigma_{ai} \sigma_{zi} \quad [\text{W sr}^{-1}]. \quad (1.a)$$

This equation may be simplified by replacing the normal irradiance E_{ni} [$\text{W (proj. cm}^2)^{-1}$] incident on each reflecting point by an average normal irradiance given by $E_{na} = \Phi_i / A_i$ [W cm^{-2}], where Φ_i [W] is the radiant flux of the incident beam and A_i is the cross-sectional area of the incident beam. This does not require that the incident beam be uniform, but only (1) that a statistically large number of reflecting points be illuminated and (2) that the incident beam be uniform enough so that no large portion of the incident flux falls on only a few reflecting points. The total radiant intensity thus becomes

$$I_T = \frac{R(s, n, k) \Phi_i \cos s}{\cos \theta} \left| J \left(\frac{\alpha, z}{\theta, \psi} \right) \right| \frac{1}{A_i} \sum_{i=1}^N \sigma_{ai} \sigma_{zi} \quad [\text{W sr}^{-1}]. \quad (2)$$

If all dependence on the surface material and laboratory geometry can be separated into one factor and all dependence on the surface structure into a second factor, this second factor would be a surface-structure function. Notice that all dependence of the surface structure is localized in the summation factor of equation (2); however, this factor contains a dependence on the laboratory geometry; namely, N varies with incidence angle β . This can be removed as follows: For normal incidence (incidence angle $\beta = 0$) and a chosen direction of reflection, consider the set of N_n reflecting points. Their curvature radii products ($\sigma_{ai} \sigma_{zi}$, $i = 1, 2, \dots, N_n$) comprise the summation factor in equation (2). As the incidence angle increases, this same set of points reflects into a new direction. The new radiant intensity is given

by equation (2) with different values of θ , ψ , a , J , etc., but with the same set of $\sigma_{ai} \sigma_{zi}$ in the summation factor. However, as the angle of incidence, β , increases, the illuminated macrosurface area increases, as $1/\cos \beta$, and some points in the additional area also contribute to the reflection. So the summation factor for the new radiant intensity must contain some additional $\sigma_{ai} \sigma_{zi}$ quantities. Assuming that the surface is statistically uniform, these extra quantities will be statistically the same as the original set, and the summation factor is merely increased by $1/\cos \beta$. Thus equation (2) becomes

$$I_T = \frac{R(s,n,k) \Phi_i \cos s}{\cos \beta \cos \theta} \left| J \left(\frac{a,z}{\theta,\psi} \right) \right| \frac{1}{A_i} \sum_{i=1}^{N_n} \sigma_{ai} \sigma_{zi} \quad [W \text{ sr}^{-1}], \quad (3)$$

and the incidence angle dependence has been separated from the summation factor. However, the summation factor still retains a dependence on the laboratory geometry, namely, N_n is proportional to the cross-sectional area A_i of the incident beam. This is easily compensated for by including the $1/A_i$ factor with the summation factor.

Thus, the quantity

$$D(a) = \frac{1}{A_i} \sum_{i=1}^{N_n} \sigma_{ai} \sigma_{zi} \quad [\text{dimensionless}] \quad (4)$$

is a surface-structure function, since it contains all the dependence on the surface structure and no dependence on anything else. In general, this quantity is a function of both the coordinates, a and z , of the microarea normal, but we are considering only surfaces whose statistical properties are directionally uniform, and for such surfaces D would have no z -dependence. In the Bouguer facet theory and its refinements, the surface-structure dependence is incorporated as a microarea-distribution function, which is the relative amount of microarea oriented in a given direction or the probability density of a facet normal to be in a given direction. Like D , this function contains all the dependence on the surface structure and no dependence on anything else. Since the two reflectance theories are identical physically, this proves that D and the microarea distribution function must be the same, or at least proportional.

Equation (3) can be put in terms of a reflectance-distribution function by dividing by the incident flux Φ_i $[W]$. This gives the PRIDF (reference 42) $f_{rls}(\beta, \theta, \psi)$ $[sr^{-1}]$. Incorporating equation (4) in addition gives

$$f_{rls}(\beta, \theta, \psi) = R(s,n,k) \frac{\cos s}{\cos \beta \cos \theta} \left| J \left(\frac{a,z}{\theta,\psi} \right) \right| D(a) \quad [W \text{ sr}^{-1}/W]. \quad (5)$$

(Division by $\sin \theta$ gives the BRDF (reference 42) $[W \text{ sr}^{-1} (\text{proj. cm}^2)^{-1}/W \text{ cm}^{-2}]$).

Average Surface Irregularity

It might prove useful if there could exist a single optically-smooth curved surface that would reflect light in the same distribution as that reflected by the ensemble of all the curved microareas comprising the rough surface. This would mean that a randomly irregular surface could be treated as if it consisted of a large number of small identical "average" irregularities or that a randomly irregular surface could be treated as if it were a single large curved surface (for a uniformly intense incident beam of the same total flux). Such an average irregularity would have to be a surface of revolution about the macrosurface normal because of the assumed directional independence of the rough surface statistics.

Mathematically, the question of the possible existence of such an average irregularity may be stated as follows. Let $\rho_a(a)$ and $\rho_z(a)$ be the radii of curvature for the average irregularity (defined as were, respectively, σ_a and σ_z , for a curved microarea), and let C be a constant. There must exist a surface of revolution whose $D(a)$, given by

$$D(a) = C\rho_a(a)\rho_z(a) \quad [\text{dimensionless}], \quad (6)$$

is the same as the $D(a)$ resulting from equation (4). It may be, but is not obvious, that for any physically realistic functional form of $D(a)$, given by equation (4), there exists a surface of revolution which, by equation (6), can give this same functional form of $D(a)$. It will be proved that this is indeed true and, furthermore, that the shape of the surface of revolution can be very greatly restricted and still be general enough to be able to give any physically realistic functional form of $D(a)$.

The following restrictions may be applied to $D(a)$ to make it conform to physical reality.

1. $D(a)$ must exist for all values of a at least between 0 and $\pi/2$. Any realistic rough surface will have some microareas at any given value of a between 0 and $\pi/2$.
2. $D(a)$ must be finite for all values of a , since no real surface would contain any perfectly flat or perfectly cylindrical microarea. (In wave optics, all flat, rough surfaces produce a perfectly specular reflection, of some magnitude. This produces a delta function in the reflectance-distribution function and thus an infinite $D(a)$ at one point. However, we are treating only ray optical reflection.)
3. $D(a)$ is positive for all values of a . This follows from equation (4), considering that σ_{zi} and σ_{ai} were defined such that they were always positive.
4. $D(a)$ must obviously be single-valued. No physical quantity can have more than one value for itself at the same point.
5. $D(a)$ is continuous. Physical quantities never have perfect discontinuities.

First, it will be proved that there exists a surface of revolution that can give not only the functional forms of $D(a)$ that might result from equation (4), but also any physically realistic functional form of $D(a)$. Let $h(x)$ be a curve that when revolved about $x = 0$ gives the surface of revolution (see figure 3). The ρ_z curvature radius is given by $\rho_z = |x|$. The ρ_a curvature radius is the radius of curvature of $h(x)$, so it is given by $\rho_a = [1 + (h')^2]^{3/2}/|h''|$ (primes indicate derivatives with respect to x). The angle a is equal to the negative slope angle of $h(x)$; that is, $a = \tan^{-1}(-h')$. Substituting these expressions into equation (6) gives

$$D[\tan^{-1}(-h')] = C|x|[1 + (h')^2]^{3/2}/|h''|. \quad (7)$$

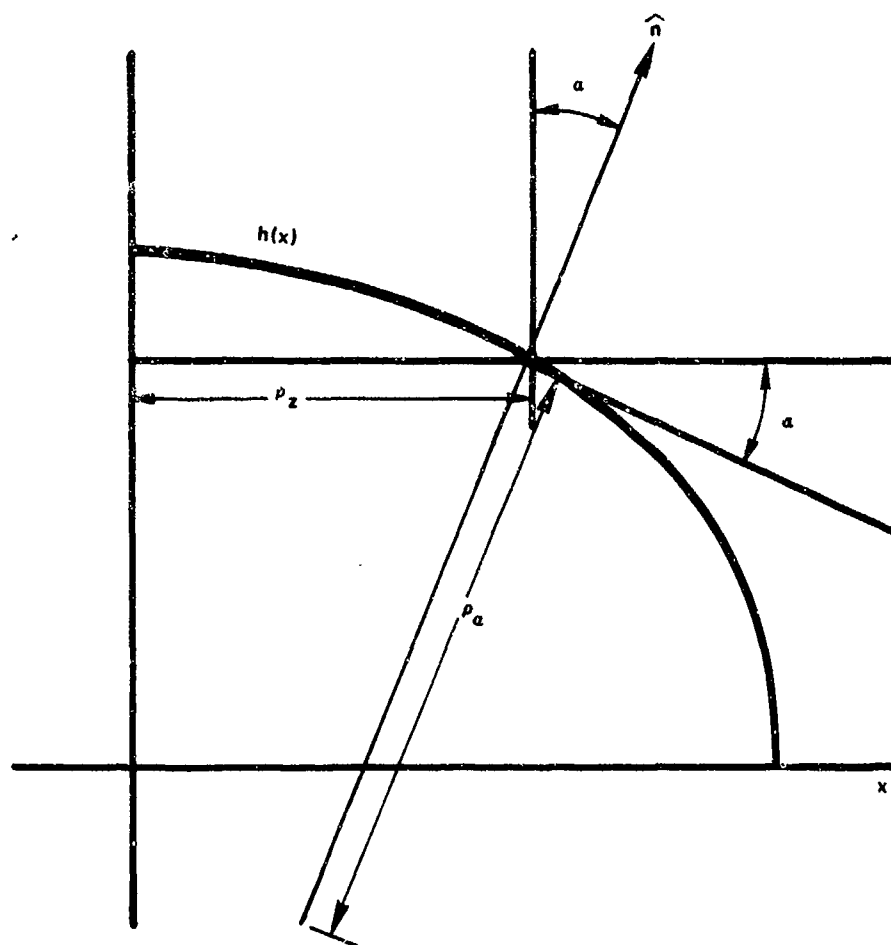


Figure 3. The Concept of an "Average" Surface Irregularity. The "average" surface irregularity is generated by rotating the curve $h(x)$ about $x = 0$. It is an optically smooth surface of revolution of a shape such that it gives the same distribution of reflected light (when irradiated by a uniform, well-collimated beam) as that given by the actual rough-surface microstructure (when irradiated by the actual, nonuniform, well-collimated beam). The shape of $h(x)$ may be restricted to the general shape shown and still be general enough to represent any microstructure. This general shape consists of the slope being zero at $x = 0$ and infinity at $h = 0$ and the curve between having no inflection points or straight-line sections.

Substitution of $p(x) = h'(x)$ gives

$$|p'|/|x| = C(1 + p^2)^{3/2}/D[\tan^{-1}(-p)], \quad (7a)$$

which is equivalent to

$$p' = Cx(1 + p^2)^{3/2}/D[\tan^{-1}(-p)], \quad p'/x \geq 0, \quad (7b)$$

$$p' = -Cx(1 + p^2)^{3/2}/D[\tan^{-1}(-p)], \quad p'/x \leq 0. \quad (7c)$$

Equations (7b) and (7c) are of the form $p' = f(x, p)$. "A differential equation of this form has a solution $p = p(x)$ through every point $(x = x_0, p = p_0)$ with a neighborhood throughout which $f(x, p)$ is continuous." Since the $f(x, p)$ of each of the above equations is everywhere continuous, all points (x_0, p_0) have

continuous neighborhoods, and a solution $p = p(x)$ to each equation exists for all values of x . Since both equations (7b) and (7c) have solutions for all values of x , equation (7a) must have a solution $p = p(x)$ for all values of x . Since

$$h(x) = \int p(x)dx + C_1$$

(C_1 is an arbitrary constant), and since $p(x)$ exists for all values of x , then $h(x)$ must exist. Thus, there must exist a solution $h = h(x)$ to equation (7) for any physically realistic $D(a)$; that is, there must exist a surface of revolution capable of representing any physically realistic rough surface.

With this established, it will now be shown that not only is there an $h(x)$ for every $D(a)$; but that also some limits to the form of $h(x)$ can be established such that $h(x)$ is still capable of giving any form of $D(a)$; that is, because of the nature of equation (7), certain options are allowed, the choice of one of which will not limit the ability of $h(x)$ to give any $D(a)$. Two options are the arbitrary choices of two boundary conditions for a second-order differential equation: one condition on $h'(x)$ and one on $h(x)$. This is allowed because a solution to a differential equation is obviously still a solution when restricted by a boundary condition, and the set of solutions $h(x)$ for all forms of $D(a)$ are obviously still solutions for their respective forms of $D(a)$ even though the same boundary condition is applied to every $h(x)$. A third option is the choice of a plus or minus sign for $h''(x)$. This is allowed because only its absolute value appears in equation (7). Thus we have established some ways of limiting the shape of the surface of revolution.

Thus far we have found two types of ways of limiting the functional form of $h(x)$ while not limiting its ability to give any physically realistic form of $D(a)$. These were three arbitrary options of restrictions on $h(x)$ resulting from the nature of equation (7) and five restrictions on $D(a)$ resulting from physical reality. These will be applied in the following way to determine a very limited type of curve for $h(x)$, but a type of curve that is still versatile enough to give any physically realistic form of $D(a)$. First, let the boundary condition on $h'(x)$ be $h'(0) = 0$. This makes the slope of $h(x)$ zero at $x = 0$. Second, use the option on the sign of $h''(x)$ to make $h''(0)$ negative. This forces the slope of $h(x)$ to begin to decrease as x begins to increase (from zero). Third, the $h(x)$ cannot have inflection points. If it did, the same value of a would occur at different parts of the curve. Since D could have different values at these two points, there would be two values of D for the one value of a . Thus D would be multiple-valued, and restriction (4) would be violated. Fourth, the $h(x)$ cannot be a straight line at any point. If it were, ρ_a would be infinite at that point and thus, by equation (6), D would be infinite, and restriction (2) would be violated. Thus far, the slope has been forced to be level (zero) at $x = 0$ and start to slope down (decrease) as x starts to increase. Since $h(x)$ can have no inflection points or straight-line segments, the slope must continue to decrease with increasing x . Thus the slope must become vertical ($-\infty$) at a finite value of x (say, x_0). If the slope only approached vertical as x approached infinity, $h(x)$ would approach a straight line and D would approach infinity, and restriction (2) would be violated (see the appendix for a rigorous verification of this contention). Last, let the boundary condition on $h(x)$ be $h(x_0) = 0$. This forces the vertically sloping part of $h(x)$ to lie on the x -axis.

In summary, a limited functional form of $h(x)$ capable of giving any physically realistic functional form of $D(a)$ resembles the curve in figure 5. This curve is level at $x = 0$, decreases with increasing x without inflection points or straight sections, and becomes vertical as it crosses the x -axis. Or, in terms of a , the curve is such that $a = 0$ at $x = 0$, and a increases without stopping or turning back with increasing x to become $a = 90^\circ$ at $h = 0$.

It is instructive to be able to visualize the random topography of a rough surface as being equivalent to one large surface of revolution of very restricted shape, but what substantive contribution does this make? It does not put any limits on the functional form of the surface-structure function $D(a)$, as we have just proved. But it may give insight into the discovery of better models to represent the surface structure. Indeed, as is shown later, the most obvious choice of a surface of revolution, an ellipsoid of

revolution, gives a surface-structure function that is better than the existing ones. Perhaps other shapes for the surface of revolution will give even better results. Also, maybe ones involving two or more parameters will give very good higher order approximations. To derive the $D(a)$ for any surface of revolution, the procedure used later for the ellipsoid can be followed.

Model in Terms of Measurable Variables

For the result, equation (5), to be useful, the unmeasurable variables α , z , and s and the Jacobian J must be found in terms of the measurable variables β , θ , and ψ . The angles α and z can be found from the reflection equation

$$\hat{r} \times \hat{n} = \hat{n} \times \hat{l} \quad (8)$$

since this is the condition that forces $\hat{n}(a, z)$ to be in a determined direction for light from a source in the direction $\hat{l}(\beta)$ to be reflected in the direction $\hat{r}(\theta, \psi)$. These three vectors are expressed as follows:

$$\hat{l} = \hat{j} \sin \beta + \hat{k} \cos \beta, \quad (9)$$

$$\hat{n} = \hat{i} \sin z \sin \alpha + \hat{j} \cos z \sin \alpha + \hat{k} \cos \alpha, \quad (10)$$

$$\hat{r} = \hat{i} \sin \psi \cos \theta + \hat{j} \cos \psi \cos \theta + \hat{k} \sin \theta. \quad (11)$$

Substituting these equations into equation (8) gives the following:

$$\cos z \sin \alpha \cos \beta - \cos \alpha \sin \beta = \cos \psi \cos \theta \cos \alpha - \sin \theta \cos z \sin \alpha, \quad (12)$$

$$-\sin z \sin \alpha \cos \beta = \sin \theta \sin z \sin \alpha - \sin \psi \cos \theta \cos \alpha, \quad (13)$$

$$\sin z \sin \beta = \sin \psi \cos \theta \cos z - \cos \psi \cos \theta \sin z. \quad (14)$$

The $\alpha(\beta, \theta, \psi)$ and $z(\beta, \theta, \psi)$ can be found by solving equations (13) and (14), respectively. Then

$$\tan \alpha = \sin \psi \cos \theta / [\sin z (\sin \theta + \cos \beta)], \quad (15)$$

$$\tan z = \sin \psi \cos \theta / (\sin \beta + \cos \psi \cos \theta). \quad (16)$$

Equation (16) gives $z(\beta, \theta, \psi)$, and if this is used in equation (15), equation (15) gives $\alpha(\beta, \theta, \psi)$. The angle s can be found by substituting equations (9) and (10) into the relation $\hat{l} \cdot \hat{n} = \cos s$:

$$\cos s = \cos z \sin \alpha \sin \beta + \cos \alpha \cos \beta. \quad (17)$$

Since $\alpha(\beta, \theta, \psi)$ and $z(\beta, \theta, \psi)$ are given by equations (15) and (16), this gives $s(\beta, \theta, \psi)$.*

*Similar expressions are derived by Torrence and Sparrow (reference 19). To compare these and other results, the following conversion between our and their symbolisms was found:

$$\begin{array}{ccccccc} \text{T \& R} & \alpha & \theta & \psi & s & a \\ \text{T \& S} & \psi & \pi/2 - \theta & \phi + \pi & \psi' & -a \end{array}$$

When equations (15), (16), and (17) were converted to the T & S symbolism and compared to the corresponding expressions of T & S, they were found to be very dissimilar in form. However, numerically they compared identically.

With the use of equations (15) and (16), the Jacobian determinant J can be evaluated:

$$J\left(\frac{a,z}{\theta,\psi}\right) = \frac{-\cos^2 z \cos^2 a \sin \psi \cos^2 \theta (1 + \sin \theta \cos \beta + \cos \theta \cos \psi \sin \beta)}{\sin z (\sin \theta + \cos \beta)^2 (\sin \beta + \cos \psi \cos \theta)^2} \quad (18)$$

This, however, was found numerically to be equal to

$$J\left(\frac{a,z}{\theta,\psi}\right) = \frac{-\cos \theta}{4 \cos s \sin a} \quad (19)$$

Although it was difficult, this equivalence was also verified analytically.

Microres Reflection Coefficient

The $R(s,n,k)$ in equation (5) can be found from the Fresnel equations (with a complex index of refraction). The reflectances R_{\perp} and R_{\parallel} for incident light linearly polarized perpendicular and parallel to the local plane of incidence, respectively, are given (references 43 and, in somewhat different form, reference 44) by the following:

$$R_{\perp}(s,n,k) = \frac{\sin^2(s - s_2) + \sinh^2 \chi}{\sin^2(s + s_2) + \sinh^2 \chi} \quad (20)$$

$$R_{\parallel}(s,n,k) = \frac{\cos^2(s + s_2) + \sinh^2 \chi}{\cos^2(s - s_2) + \sinh^2 \chi} \quad (21)$$

where

$$\sinh^2 \chi = -\frac{1}{2} c + \left(\frac{1}{4} c^2 + b^2\right)^{1/2},$$

$$\cos s_2 = b/\sinh \chi,$$

with

$$b = k \sin s / (n^2 + k^2),$$

$$c = 1 - \sin^2 s / (n^2 + k^2).$$

and n and k , respectively, the real and imaginary components of the complex index of refraction of the surface material. The k is sometimes called the absorption index of the surface material. Of academic interest are s_2 and χ , which come from Snell's Law for a complex index of refraction.

$$\sin s / \sin(s_2 + i\chi) = n - ik$$

At $s = 0$, equations (20) and (21) are indeterminate. However, the solutions are found (reference 45) to be

$$R_{\perp}(0, n, k) = R_{\parallel}(0, n, k) = \frac{n^2 + k^2 + 1 - 2n}{n^2 + k^2 + 1 + 2n} \quad (22)$$

The above expressions give R for light polarized relative to the local plane of incidence; however, for laboratory measurements R must be determined for light polarized relative to the macroscopic plane of incidence, since this is the usual way that the incident polarization is specified. The angle between the macroscopic and local planes of incidence ϕ is the angle between their respective normals, \hat{i} and $\hat{i} \times \hat{n}$ (see figure 4), so ϕ is given by

$$\cos \phi = \hat{i} \cdot \hat{i} \times \hat{n} / \sin s.$$

Substituting equations (9) and (10) into the above equation gives

$$\cos \phi = (\sin \beta \cos \alpha - \cos \beta \cos \gamma \sin \alpha) / \sin s, \quad (23)$$

for which everything on the right-hand side has been found. The orientation of the incident polarization plane is specified by the angle γ , the angle that the incident polarization plane makes with the macroscopic plane of incidence. The angle $\gamma - \phi$ is then the angle that the incident polarization plane makes with the local plane of incidence. For calculation of the reflectance of the incident light, its polarization must be resolved into components perpendicular and parallel to the local plane of incidence. A part $\sin^2(\gamma - \phi)$ of the incident light is polarized perpendicular to the local plane of incidence for which the reflectance is $R_{\perp}(s)$, and a part $\cos^2(\gamma - \phi)$ of the incident light is polarized parallel to the local plane of incidence for which the reflectance is $R_{\parallel}(s)$. Thus the reflectance of light polarized at an angle γ from the macroscopic plane of incidence is

$$R(s, \gamma) = R_{\perp}(s) \sin^2(\gamma - \phi) + R_{\parallel}(s) \cos^2(\gamma - \phi) \quad (24)$$

From this, the reflectance of light polarized parallel and perpendicular to the macroscopic plane of incidence is given by

$$R_V(s) = R(s, \gamma = 0) = R_{\perp}(s) \sin^2 \phi + R_{\parallel}(s) \cos^2 \phi,$$

and

$$R_H(s) = R(s, \gamma = \pi/2) = R_{\parallel}(s) \cos^2 \phi + R_{\perp}(s) \sin^2 \phi,$$

respectively

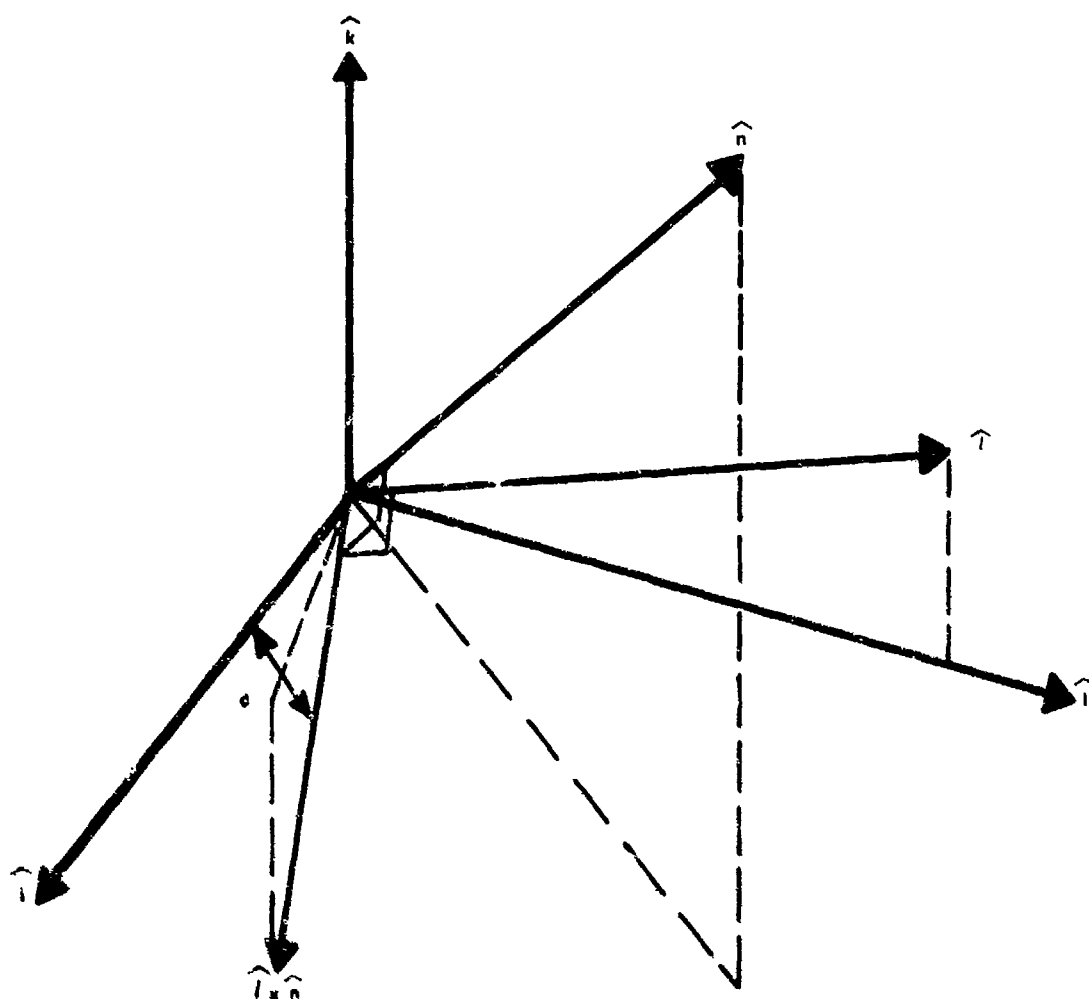


Figure 4. Relation Between the Local and Macrosurface Plane of Incidence. The vectors \hat{i} and \hat{h} lie in the macrosurface plane of incidence, and \hat{i} and \hat{n} lie in the local plane of incidence. The angle between these planes is equal to ϕ (the angle between their normals).

The reflectance $R_{\perp}(s)$ of unpolarized or circularly polarized light, is simply the average of $R_{\perp}(s)$ and $R_{\parallel}(s)$, since both unpolarized and circularly polarized light resolve into equal components perpendicular and parallel to the local plane of incidence

$$R_{\perp}(s) = \frac{1}{2} [R_{\perp}(s) + R_{\parallel}(s)]$$

The above equations reveal no information on the polarization form of the reflected light. If the reflected polarization form is desired, from Holl (reference 44), the phase shift difference δ between R_{\perp} and R_{\parallel} is given, and from Shurcliff (reference 46), the Mueller matrix (containing R_{\perp} , R_{\parallel} , δ , and ϕ) for the polarization transformation on reflection can be derived

Normalization

Substituting equations (19) and (6) into equation (5) gives

$$f_{\text{rls}}(\beta, \theta, \psi) = R(s, \gamma, n, k) \frac{1}{4 \cos \beta} \frac{C \rho_a(a) \rho_z(a)}{\sin a} [W \text{ sr}^{-1}/W]. \quad (25)$$

As follows, the constant C can be found so as to make the reflected intensity-distribution function f_{rls} an absolute quantity. Since the average irregularity is a surface of revolution, the region around $a = 0$ can be treated as a spherical mirror surface of radius $\rho_a(0)$. For normal incidence and reflection, it is easy to derive the BRIDF for a spherical mirror. This, of course, must be equal to the BRIDF of our model for normal incidence and reflection $f_{\text{rls}}(0^0, 90^0, 0^0)$, and C can be found from this equality.

The focal length of a spherical mirror is equal to half the radius, or $\frac{1}{2}\rho_a(0)$, and collimated incident light reflects into a cone with the focal point as its vertex. A flux of $(\Phi_1/A_1) \Delta A$ [W] is incident on a small area ΔA on the top of a hemisphere. If the single large surface of revolution is to replace all the illuminated areas of the real surface, it must have uniformly intense light incident on all parts of it and have no light missing it. Therefore, the area of its base $\pi \rho_z^2(\pi/2)$ [cm²] must equal the incident beam cross-sectional area A_1 , and thus $\Phi_1 \Delta A / (\pi \rho_z^2(\pi/2))$ [W] is the flux incident on ΔA . Upon reflection, this flux is attenuated by $R(0)$ and is diverged into $\Delta A / [\frac{1}{2}\rho_a(0)]^2$ steradians. Then $R(0)$ multiplied by the above incident flux and divided by this number of steradians gives the reflected radiant intensity [W sr⁻¹]. Additionally dividing this by Φ_1 [W] gives the BRIDF for the spherical mirror:

$$f_{\text{rls}}(0^0, 90^0, 0^0) = R(0) \rho_a^2(0) / [4\pi \rho_z^2(\pi/2)] [W \text{ sr}^{-1}/W] \quad (26)$$

For the rough-surface model at normal incidence and reflection, $\beta = 0$, $\theta = \pi/2$, $a = 0$, $s = 0$, and $\rho_z(0) = 0$ occur, and equation (25), the BRIDF becomes

$$f_{\text{rls}}(0^0, 90^0, 0^0) = \frac{1}{4} C R(0) \rho_a(0) \lim_{a \rightarrow 0} (\rho_z(a) / \sin a) [W \text{ sr}^{-1}/W]. \quad (27)$$

Equating equations (26) and (27) and solving for the normalization constant C gives

$$C = \rho_a(0) / [\pi \rho_z^2(\pi/2) \lim_{a \rightarrow 0} (\rho_z(a) / \sin a)]. \quad (28)$$

Substituting this into equation (25) gives the normalized or absolute form for the BRIDF.*

$$f_{rls}(\beta, \psi) = R(s, \gamma, n, k) \frac{1}{4\pi \cos \beta} \frac{\rho_a(0) \rho_a(a) \rho_z(a)}{\rho_z^2(\pi/2) \lim_{a \rightarrow 0} (\rho_z(a)/\sin a) \sin a} [W \text{ sr}^{-1}/W] \quad (29)$$

Ellipsoid of Revolution Average Surface Irregularity Approximation

It is not practicable to make direct measurements of the σ_{ai} and σ_{zi} values or of $\rho_a(a)$ and $\rho_z(a)$. The best that one can do is to choose a reasonable model irregularity. A sphere is one possibility, but it contains no parameter that one can vary to change the characteristics of the surface structure. An ellipsoid of revolution, $h = e(1 - x^2)^{1/2}$, has one such parameter e , which is the ratio of the length of the axis-rotated-about to the length of the axis-rotated. As e decreases, the model irregularity becomes flatter and reflects more light in the specular direction. This is a very useful property, since the wide variety of real surfaces contains a continuous distribution of diffuse-to-highly-specular surfaces. The $f_{rls}(\beta, \psi)$ for the ellipsoid of revolution is found by evaluating equation (29) as follows. The derivative of $h(x)$ for the ellipsoid is

$$h' = -ex(1 - x^2)^{-1/2} = -\tan a.$$

Solving for x gives

$$x = \tan a (\tan^2 a + e^2)^{-1/2} = \rho_z(a)$$

The second derivative of $h(x)$ is

$$h'' = -e(1 - x^2)^{-3/2} = -e[1 - \tan^2 a / (\tan^2 a + e^2)]^{-3/2}.$$

The $\rho_a(a)$ is the radius of curvature of $h(x)$ and is thus given by $\rho_a(a) = [1 + (h')^2]^{3/2}/|h''|$. Substituting h' and h'' this equation gives

$$\rho_a(a) = e^2 [(1 + \tan^2 a)/(e^2 + \tan^2 a)]^{3/2}.$$

The other components of equation (29) are found to be:

$$\rho_a(0) = 1/e; \rho_z(\pi/2) = 1; \text{ and } \lim_{a \rightarrow 0} [\rho_z(a)/\sin a] = 1/e.$$

Substituting the above expressions into equation (29) gives the BRIDF (reference 42) for the ellipsoid of revolution—average irregularity.

*One could extend this model to include shadowing by simply multiplying equation (29) by Torrance and Sparrow's shadowing factor (symbolism converted by use of the table in the footnote following equation (17)). This would not affect the normalization, since their shadowing factor is normalized to equal one when no shadowing occurs.

$$f_{rls}(\beta, \theta, \psi) = \frac{R(s, \gamma, n, k)}{4\pi \cos \beta} \frac{e^2}{(e^2 \cos^2 \alpha + \sin^2 \alpha)^2} [W \text{ sr}^{-1}/W] \quad (30)$$

(Division by $\sin \theta$ gives the BRRDF $[W \text{ sr}^{-1} (\text{proj. cm}^2)^{-1}/W \text{ cm}^{-2}]$.)

Thus, with equation (30) we have a simple model giving the absolute BRIDF contributed by ray reflection from the irregular microsurface.* Only three parameters are involved: the refractive index n of the surface material, the absorption index k of the surface material, and the axis ratio e of the ellipsoid of revolution—average surface irregularity representing the surface structure. All other quantities in equation (30) have been found in terms of the laboratory coordinates β, θ , and ψ .

COMPARISON TO MEASUREMENTS

Earlier, we speculated that the concept of an average surface of revolution representing the surface structure might give insight into the choice of a better surface-structure function. The first choice, the ellipsoid of revolution, resulted in the surface-structure function given by the last term in equation (30). Normalized to $D(\alpha = \theta) = 1$, it is

$$D(\alpha) = e^4 / (e^2 \cos^2 \alpha + \sin^2 \alpha)^2. \quad (31)$$

Since this surface-structure function was shown to be equivalent to the microarea distribution function used as the surface-structure function in the Bouguer facet theory, this function can be compared directly to the others. Rense (reference 21) found a way to determine the microarea distribution function from the reflectance-distribution function measurements. Figure 5 presents his data for one rough surface, along with plots of best fits for our structure function and three microarea distribution functions found in the literature. The much closer fit to the data shows our function to be a significant improvement.

To test the accuracy of the model, to illustrate the value of the concepts derived, and to test the applicability of the model to laser target designation systems, the model was combined as follows with some Lambertian reflection and compared to BRIDF measurements made on a variety of rough surfaces.

The BRIDF contributed by the Lambertian reflection is simply given by

$$f_{rlL}(\beta, \theta, \psi) = \sin \theta \rho_L(\beta, 2\pi)/\pi [sr^{-1}], \quad (32)$$

where $\rho_L(\beta, 2\pi)$ [Lambertian directional-hemispherical reflectance (references 42 and 47)] is the portion of the incident power scattered by Lambertian reflection. This quantity might vary significantly with incidence angle, but for lack of any relationship, it will be assumed constant. This is added to equation (30) to give the combined BRIDF:

$$f_{rl}(\beta, \theta, \psi) = f_{rls}(\beta, \theta, \psi) + f_{rlL}(\beta, \theta, \psi) [sr^{-1}]. \quad (33)$$

*Equation (30) was found to compare to Torrence and Sparrow's result. To compare the two results, our symbolism was transformed, the two surface structure functions were made equal to one, T&S's shadowing factor was removed, and the BRIDF was transformed to T&S's ratio of BRRDF's. This completed, the results were the same.

○ Data taken from Rense (reference 21)

———— Plot of our function $e^4/(e^2 \cos^2 \alpha + \sin^2 \alpha)^2$ ($e = 0.40$)

..... Plot of function $e^2/(e^2 \cos^2 \alpha + \sin^2 \alpha)$ ($e = 0.25$), originated by Berry (reference 13)

----- Plot of function $(\cos^{-4} \alpha) \exp(-A^2 \tan^2 \alpha)$ ($A^2 = 7.62$) derived from Beckmann's (reference 28) result for a surface characterized by a Gaussian distribution of surface heights and an autocorrelation length in the ray optics approximation

----- Plot of function $(\cos^{-2} \alpha) \exp(-A^2 \tan^2 \alpha)$ ($A^2 = 6.93$) used by Sirohi (reference 22), originated by Berry (reference 13)

----- Plot of an approximation $\exp(-A^2 \alpha^2)$ ($A^2 = 0.0021/\text{degrees}^2$) of ----- used by Rense (reference 21) for small values of α

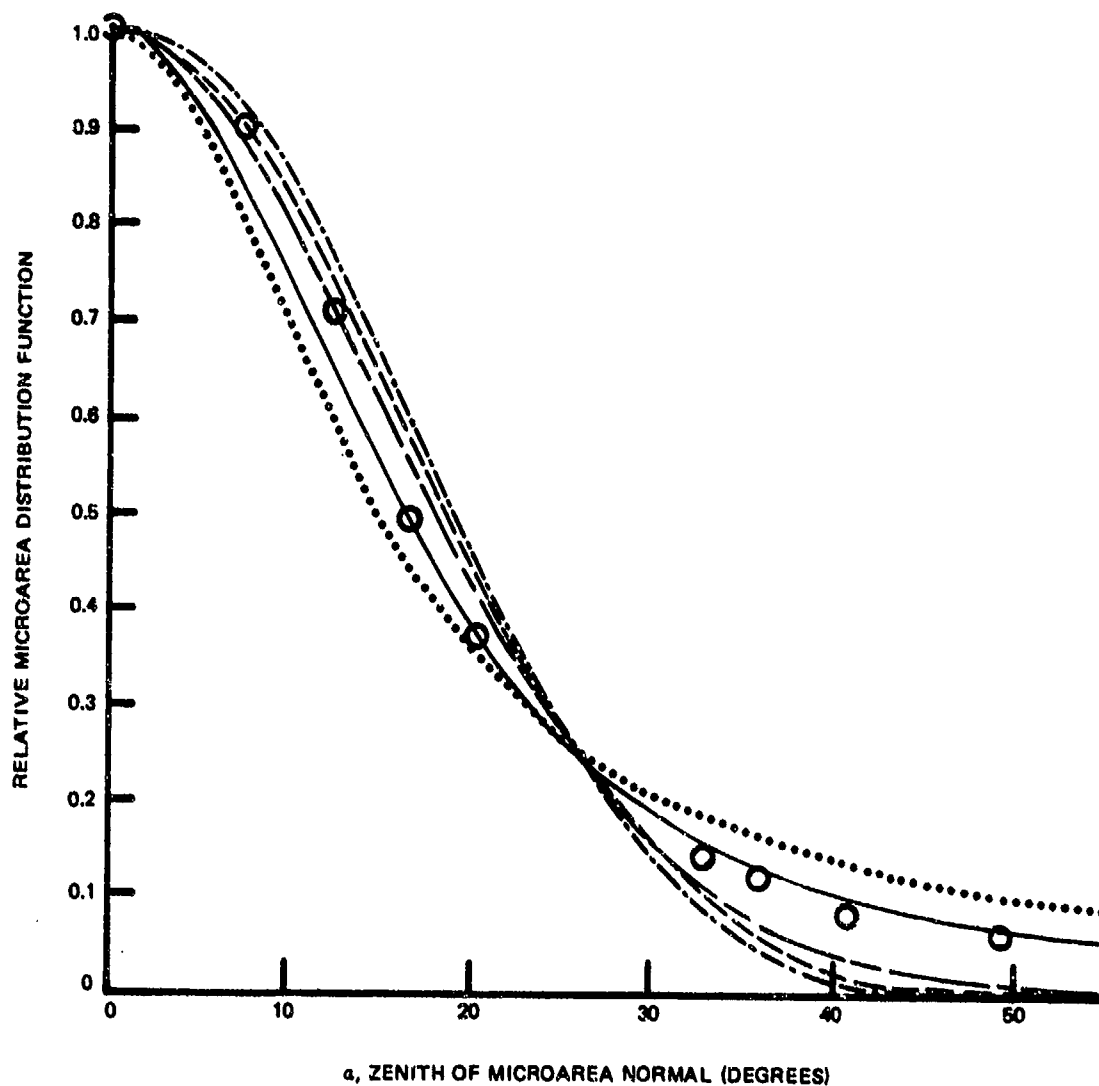


Figure 5. Comparison of Best Fits of Some Surface-Structure Functions (Equivalent to the Microarea or Facet Distribution Function).

A trial and error optimization procedure was applied to relative BRIDF measurements made on a number of surfaces. This optimization procedure consisted of a method of varying the four parameters $[e, n, k, \text{ and } \rho_L(\beta/2\pi)]$ of the model (equation 33) until the minimum value σ_m was found for σ , which is the root mean square normalized deviation of the experimental values from the theoretical values.

$$\sigma = \left\{ \frac{1}{M} \sum_{i=1}^M \left[\left(\frac{f_{rli} - c X_i}{f_{rli}} \right)^2 \right] \right\}^{1/2}$$

where

$$c = \left(\sum_{i=1}^M f_{rli} \right) / \left(\sum_{i=1}^M X_i \right);$$

X_i is measured relative value of relative BRIDF; f_{rli} is the theoretical value; and M is the number of measurements on a given surface. The set of measurements for each surface consisted of the following. For each combination of values of θ of 15, 30, 45, 60, 75, and 90 degrees and of β of 0, 15, 30, 45, 60, and 70 degrees, several values of ψ were chosen, and the relative BRIDF was measured for collimated 6.328-Angstrom continuous wave laser light polarized perpendicular and parallel to the plane of incidence. This resulted in about 400 measurements for each surface. This number is statistically large, so the location of σ_m in the space of the four parameters should not be sensitive to small random experimental errors.

Table 1 gives σ_m and the corresponding (optimum) values of the parameters for each surface.

Figure 6 compares a small sample of the measurements to the model. A brief description of each surface and a discussion of the results is given in the following paragraphs.

The 3M Black Velvet paint is a very dull antireflection paint for optical instruments. The optimization resulted in two very nearly equal minima of σ . The associated two sets of values for the parameters of the model give nearly identical reflection patterns; therefore, reflection patterns are plotted, in figure 5, for only the first set of parameters listed in table 1. The model applied quite well. The curves compared very well with the measured points in shape and magnitude. Only the dependence on incident

Table 1. Optimum Values of the Model Parameters

Parameter	3M Black Velvet Paint		Dirtied Olive Drab Paint	Cement	Plywood	Grass
σ_m	0.290*	0.293*	0.345	0.200	0.186	0.328
ρ_L	0.020	0.022	0.06	0.33	0.40	0.5
e	0.89	0.88	0.24	0.68	0.51	1.6
n	1.50	1.52	1.0	1.00	0.9	0.7
k	0.00	0.3	0.4	0.9	1.9	1.3

*Two minima for σ were found.

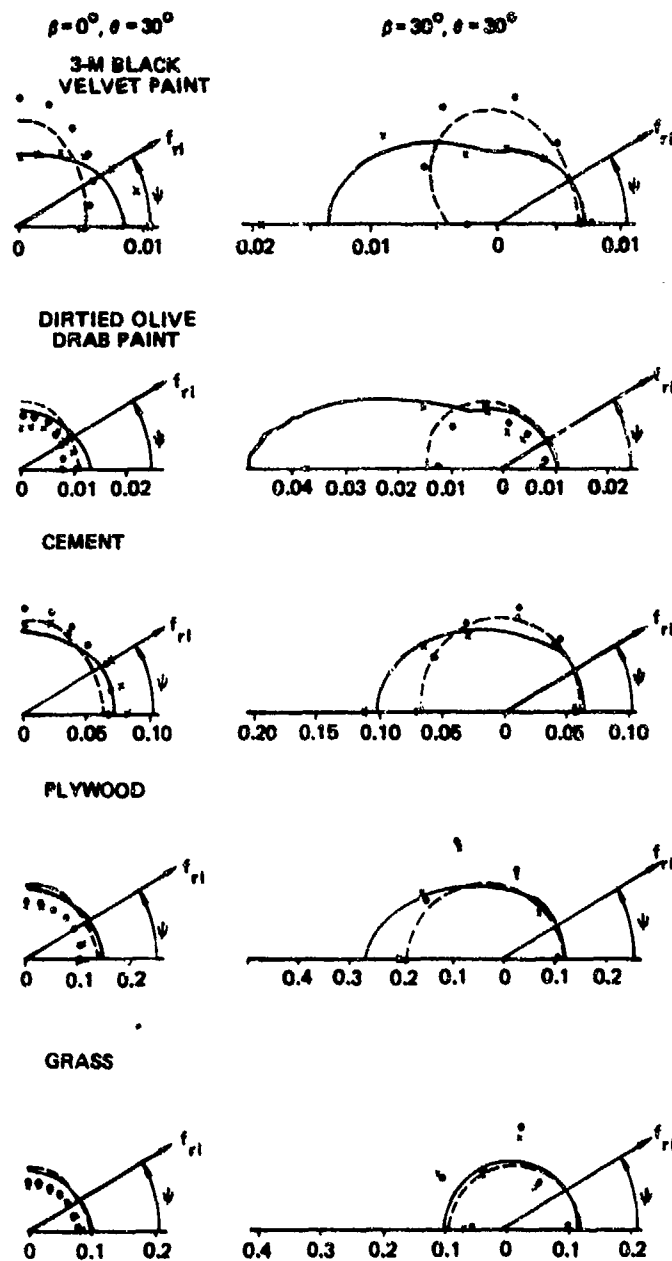
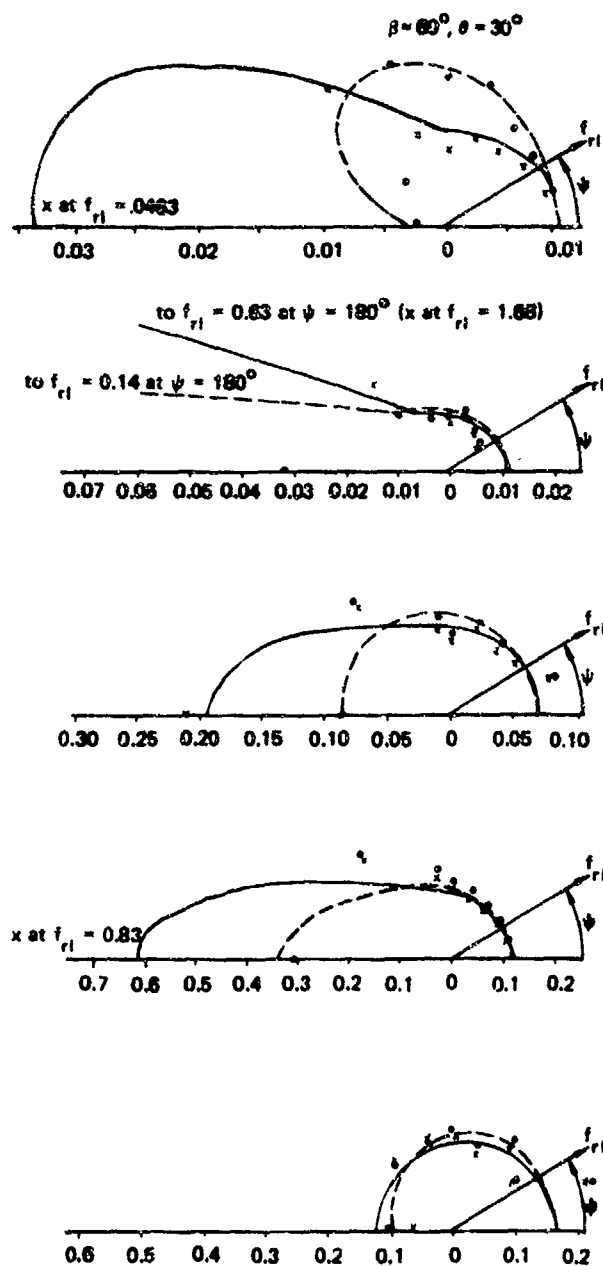


Figure 6. Comparison of Some Theoretical and Measured Values of BRIDF for a Variety of Flat Rough Surfaces. Linearly polarized, collimated, 6,328-Angstrom, continuous-wave laser light was incident at an angle β from the surface normal. The radiometer (unpolarized) observed the entire illuminated area of the surface from an elevation angle θ above the surface and from an azimuth angle ψ from the plane of incidence. On the plots, the BRIDF (reference 42) $f_{r1}(\beta, \theta, \psi)$ (reflected flux per steradian per incident flux) is given



by the radius vector from the origin to the point or curve, and ψ is given by the polar angle. [The BRDF (reference 42), reflected radiance per incident irradiance, is given by $f_{r1}/\sin \theta$.] Values for β and θ for each column of graphs are given at the top. The symbols x and \odot indicate measured values of f_{r1} , and the continuous solid and dashed curves give the theoretical plots of f_{r1} for the incident light polarized respectively perpendicular and parallel to the plane of incidence.

polarization gave a consistent error. However, this error was small for most points. Also, from the absolute values of BRIDF given by the model, the directional-hemispherical reflectance (sum of flux scattered in all directions per incident flux from one direction) at normal incidence can be estimated and was found to be of the order of magnitude of 4 percent. This is consistent with the measured directional-hemispherical reflectance value of 2.5 percent. Also, under a microscope, the surface appeared as an irregular pile of little spheres, which is consistent with the optimum ellipsoid axis ratio of $e = 0.89$, which is very nearly that of a sphere ($e = 1$). The difference could be caused by the sphere sagging slightly into ellipses when they were still liquid.

The dirtied olive drab paint was a sample of a slightly glossy dark olive drab paint. It was soiled by placing dry soil on its slightly dampened surface and shaking off all that would not stick. The model applied rather poorly. The shapes of the curves and the dependence on incident polarization were only roughly similar, and the magnitude was systematically erroneous for many curves. However, the directional-hemispherical reflectance at normal incidence, estimated from the absolute values of BRIDF given by the model, is of the order of 5 percent, which is consistent with the measured value of 4 percent. Also, the ellipsoid axis ratio e is very small, as it should be for a glossy surface; that is, a glossy surface should have a large portion of its microsurface area with normals near the microsurface normal, as does a very flat ellipsoid of revolution. Much of the poor performance of the model might be because there are two types of reflecting surfaces: the paint and the soil. The optimization assumed only one.

The cement surface consisted of common structural concrete cement troweled flat and allowed to harden in a horizontal position. The surface appeared to be slightly varied in shades of light grey. The model applied very well. There were no systematic errors. The small random errors could easily be attributed to the varied nature of the surface, since the illuminated area of the surface was not necessarily the same for each measurement. This is consistent with the fact that no such random errors occurred during the parts of the measurement program in which the illuminated area remained the same. The illuminated area remained the same for only cases in which either the incident polarization was varied or when ψ was varied at $\beta = 0$. The directional-hemispherical reflectance at normal incidence, estimated from the absolute values of BRIDF given by the model, is of the order of 50 percent, which is consistent with measured values ranging from 30 to 50 percent for various samples of concrete.

The plywood surface was clean and unaged. It had an irregular grain whose width was about equal to the diameter of the laser beam. A large portion of the grain was oriented nearly parallel to the fibers of the wood. Throughout the measurements, the plane of incidence remained parallel to the fibers. The model applied fairly well. The directional-hemispherical reflectance at normal incidence, estimated from the absolute values of BRIDF given by the model, is of the order of 70 percent, which is reasonable, since the surface appears to be highly reflecting. Also, the lowest σ_m of any surface occurred, and the grainy nature of the surface could easily account for the little remaining deviation if the deviation were random. However, much of the deviation causing σ_m was systematic. The dependence on incident polarization did not compare very well, and the experimental points deviated in the form of a bulge whose maximum appeared to shift from $\psi = 90^\circ$ to $\psi = 180^\circ$ as β varied from 0 to 90 degrees. This type of systematic error would result from this particular directional dependence of this surface's microstructure.

The grass surface was a piece of sod with fine, densely spaced blades of grass. The blades were not small enough relative to the laser-beam diameter to avoid a large random error in the measurements. Thus, only the statistical properties of the measurements are significant. The large σ_m is probably due mostly to this random error. However, a significant systematic error was discernible. Also, from the absolute values of BRIDF given by the model, the directional-hemispherical reflectance at normal incidence was estimated to be of the order of 60 percent, which is inconsistent with the 5 to 20 percent measured for several samples of grassy meadow. However, a value of e much larger than unity is realistic; that is, the surfaces of the blades of grass tend to be vertical, resulting in a concentration of the microsurface area at high angles from the macrosurface, and the model irregularity with an e greater than 1 also has this property.

For all the surfaces, the optimization gave large values for k ; greater than 0.3. Such values occur only for metals (reference 44), and these surfaces are obviously dielectric. Even a value of k of only 0.01 occurs (reference 5) only for an extremely highly absorbing dielectric such as black glass, in which 95 percent of the energy is absorbed while traveling a distance of only 25 wavelengths. In one paper (reference 48), optimization involving k resulted in zero values for dielectrics. In the present optimization (finding the values of the parameters giving the minimum overall deviation between theoretical and experimental data), a trough of minima was found in the space of the parameters n and k . For each surface, the bottom of this trough was nearly level, making the $n-k$ optimization somewhat uncertain. Also, this trough intersected the $k = 0$ axis. It is possible that the position of the minimum found along the trough for each surface was a random occurrence resulting from random errors in the experimental data and that the actual minimum was at $k = 0$. For one surface, the 3M Black Velvet, two minima were found, one at $k = 0$.

Summarizing the comparison of the model to the measurements, it has been shown that the comparison is in general reasonably good and that discrepancies can be mostly explained by the existence of gross deviations of some of the measured surfaces from the assumed surface, such as the existence of two reflecting surface materials instead of just one and the existence of a significant directional dependence of the surface structure. Since most of the data were taken outside the plane of incidence, these results tend to verify, outside the plane of incidence, the ability of interface plus Lambertian reflection to give most of the reflection in most directions for most surfaces. Also, it has been shown that the ellipsoid of revolution average surface irregularity is a useful concept, since (1) for many surfaces, one can visualize the ellipticity of the representative ellipsoid, and (2) the ellipsoid gives an improved surface structure function. Last, there has been some verification of the correctness of the normalization, since the optimization was done on relative data, and the results usually gave absolute directional-hemispherical reflectances comparable to typical measured values.

CONCLUSIONS

The following significant conclusions may be drawn about the ray-optics theory of light reflection from a rough, air/material interface.

1. The facet representation of the rough interface must give the same reflection as the actual interface, which is made up of curved surfaces.
2. For any given rough surface, there exists a single optically smooth curved surface of revolution (average irregularity) of very restricted shape that will reflect light in the same distribution as that reflected by the rough interface.

3. Modeling this average irregularity as an ellipsoid of revolution gives a surface structure function that is much more accurate and useful than previously existing ones.
4. There now exists a reflectance model that can be normalized giving a reflectance-distribution function that is absolute, and the normalization has been verified experimentally.
5. The combination of ray reflection from the rough interface plus some Lambertian reflection applies rather well outside the plane of incidence as well as within it for a variety of commonly occurring rough surfaces.

REFERENCES

1. Terminology and symbolism for radiometric quantities will be used throughout this report as proposed by J. J. Muray, F. E. Nicodemus, and I. Wunderman, Proposed Supplement to the SI Nomenclature for Radiometry and Photometry, Appl. Opt., Vol. 10 (1971), p. 1465.
2. Look, Jr., D. C. Diffuse Reflection from a Plane Surface, J. Opt. Soc. Am., Vol. 55 (1965), p. 1628.
3. Carmer, D. C., and Max E. Bair. Some Polarization Characteristics of Magnesium Oxide and Other Diffuse Reflectors, Appl. Opt., Vol. 8 (1969), p. 1597.
4. Renau, J., P. K. Cheo, and H. G. Cooper. Depolarization of Linearly Polarized Electromagnetic Waves Backscattered from Rough Metals and Inhomogeneous Dielectrics, 25 Aug 1966, Bell Telephone Laboratories, Inc., Murray Hill, N. J.
5. Schmidt, R. N., P. M. Treuenfels, and E. J. Meeham. Application of Mie Scatter Theory to the Reflectance of Paint-Type Coatings. ASME Symposium on Thermophysical Properties, 4th Proceedings (14 Apr 1968), p. 256.
6. Ivanov, A. P., and A. S. Toporets. Investigation of Diffuse Reflection by Means of Polarized Light. I, SOV PHYS TECH PHYS, Vol. 1 (1956), p. 589.
7. Minnaert, M. "Photometry of the Moon," in *Planets and Satellites, The Solar System*, edited by G. P. Kuiper and B. M. Middlehurst, Vol. 3 (University of Chicago Press, 1961), p. 229.
8. Fessenkov, V. G. "Photometry of the Moon," in *Physics and Astronomy of the Moon*, edited by Z. Kopal (Academic Press, New York, 1962), p. 113.
9. van Diggelen, J. Photometric Properties of Lunar Crater Floors, Rech. Obs. Utrecht, Vol. 14 (1959), p. 53.
10. Chandrasekhar, S. *Radiative Transfer* (Dover, New York, 1960), p. 147.
11. Hapke, B. W. A Theoretical Photometric Function for the Lunar Surface, J. Geophys. Res., Vol. 68 (1963), p. 4571.
12. Bouguer. Histoire de l'Academie Royale des sciences, Paris, 1757 (1762), and Traite d'optique sur la gradation de la lumière (ouvrage posthume de M. Bouguer, et publié par M. l'Abbe de Lacaille), Paris, 1760.

13. Berry, E. M. Diffuse Reflection of Light from a Matte Surface, *J. Opt. Soc. Am.*, Vol. 7 (1923), p. 627.
14. Pokrowski, G. I. Zur Theorie der diffusen Lichtreflexion, *Z. Physik*, Vol. 30 (1924), p. 66.
15. ———. Zur Theorie der diffusen Lichtreflexion. IV., *Z. Physik*, Vol. 36 (1926), p. 472.
16. Barkas, W. W. Analysis of Light Scattered from a Surface of Low Gloss into Its Specular and Diffuse Components, *Proc. Phys. Soc. (London)*, Vol. 51, (1939), p. 274.
17. Middleton, W. E. K., and A. G. Mungall. The Luminous Directional Reflectance of Snow, *J. Opt. Soc. Am.*, Vol. 42 (1952), p. 572.
18. Christie, A. W. The Luminous Directional Reflectance of Snow, *J. Opt. Soc. Am.*, Vol. 43, (1953), p. 621.
19. Torrance, K. E., and E. M. Sparrow. Theory for Off-Specular Reflection from Roughened Surfaces, *J. Opt. Soc. Am.*, Vol. 57 (1967), p. 1105.
20. Schulz, H. Untersuchungen über die Reflexion an teilweise lichtzerstreuenden Flächen, *Z. Physik*, Vol. 31 (1925), p. 496.
21. Rense, W. A. Polarization Studies of Light Diffusely Reflected from Ground and Etched Glass Surfaces, *J. Opt. Soc. Am.*, Vol. 40 (1950), p. 55.
22. Sirohi, R. S. Optical Constants of Rough Surface by Ellipsometry, *J. Phys. D.*, Vol. 3 (1970), p. 1407.
23. Oetking, P. Photometric Studies of Diffusely Reflecting Surfaces with Applications to the Brightness of the Moon, *J. Geophys. Res.*, Vol. 71 (1966), p. 2505.
24. McCoyd, G. C. Polarization Properties of a Simple Dielectric Rough-Surface Model, *J. Opt. Soc. Am.*, Vol. 57 (1967), p. 1345.
25. Pokrowski, G. I. Zur Theorie der diffusen Lichtreflexion, II, *Z. Physik*, Vol. 35 (1925), p. 34.
26. Planck, Max. *The Theory of Heat Radiation* (Dover, New York, 1959).
27. Jones, R. C. Appendix to Spiro, Jones, and Wark, *Infrared Phys.*, Vol. 5 (1965), p. 11.
28. Beckmann, P., and A. Spizzichino, *The Scattering of Electromagnetic Waves from Rough Surfaces* (MacMillan, New York, 1963).
29. Ibid., p. 5.
30. Voishvillo, N. A. Reflection of Light by a Rough Glass Surface at Large Angles of Incidence of the Illuminating Beam, *Opt. Spectrosc.*, Vol. 22 (1967), p. 517.
31. Toponets, A. S. Specular Reflection from a Rough Surface, *Opt. Spectrosc.*, Vol. 16 (1964), p. 54.
32. Polyanski, V. K., L. V. Kovalski, and T. I. Milovidova. Specular Reflection from a Mat Surface with Coarse Microtopography, *Opt. Spectrosc.*, Vol. 25 (1968), p. 415.

33. Polyanskii, V. K., and V. P. Ryachev. On the Reflection of Light from Rough Surfaces, *Opt. Spectrosc.*, Vol. 20 (1966), p. 391.
34. ----- Scattering of Light Reflected from Statistically Distributed Microareas. *Diffraction Study*, *Opt. Spectrosc.*, Vol. 22 (1967), p. 152.
35. Polyanskii, V. K. The Radiation Scattering Matrix of a Mat Surface in the Diffraction Approximation, *Opt. Spectrosc.*, Vol. 24 (1968), p. 531.
36. Fung, A. K. On Depolarization of Electromagnetic Waves Backscattered from a Rough Surface, *Planet. Space Sci.*, Vol. 14 (1966), p. 563.
37. Gorodinskii, G. M. Polarizing Properties of Frosted Glass Surfaces in the Case of Reflection, *Opt. Spectrosc.*, Vol. 16 (1964), p. 59.
38. Richmond, J. C. Effect of Surface Roughness on Emittance of Nonmetals, *J. Opt. Soc. Am.*, Vol. 56 (1966), p. 253.
39. Umov, N. A. *Selected Works* (State Publishers of Technical-Theoretical Literature, 1950).
40. Nicodemus, F. E. Reflectance Nomenclature and Directional Reflectance and Emissivity, *Appl. Opt.*, Vol. 9 (1970), p. 1474.
41. ----- Radiance, *Am. J. Phys.*, Vol. 31 (1963), p. 368.
42. Ginsberg, Limperis, Nicodemus, and Richmond. "Geometrical Considerations for Reflectance Nomenclature." In preparation as a National Bureau of Standards Technical Note. (Received as a private communication from F. E. Nicodemus, Naval Weapons Center, China Lake, California.)
43. Holl, H. B. "The Reflection of Electromagnetic Radiation," Vol. I, Army Missile Command (U.S.) Report No. AF-TR-63-4 (1963).
44. ----- Specular Reflection and Characteristics of Reflected Light, *J. Opt. Soc. Am.*, Vol. 57 (1967), p. 683.
45. Born, M., and E. Wolf. *Principles of Optics* (MacMillan, New York, 1964), p. 620.
46. Shurecliff, W. A. *Polarized Light* (Harvard University Press, Cambridge, Mass., 1966).
47. Judd, D. B. Terms, Definitions, and Symbols in Reflectometry, *J. Opt. Soc. Am.*, Vol. 57 (1967), p. 445.
48. Treat, C. H., and M. W. Wildin. *Progress in Astronautics and Aeronautics*, Vol. 23 (Academic Press, New York, 1970), p. 77.

APPENDIX
PROOF THAT x IS FINITE WHEN
THE SLOPE OF $h(x)$ IS VERTICAL

The contention that x is still finite when the slope of $h(x)$ is vertical can be more rigorously verified by the following derivation of the upper bound x_0 on the value of x at which $h'(x) = \infty$. Equation (7) can be rewritten as

$$h''(x) = -Cx [1 + (h')^2]^{3/2}/D(a),$$

which upon integration gives a monotonically decreasing function $h'(x)$ provided that $0 < D(a) < \infty$. A lower bound on $|h''(x)|$ is given from

$$|h''(x)| \geq Cx h'^3/D^*,$$

where D^* is the upper bound on $D(a)$. Since both $h'(x)$ and $h''(x)$ are negative, we have

$$h''/(h')^3 \geq Cx/D^*,$$

which upon integration gives

$$1/(h'_2)^2 \leq 1/(h'_1)^2 + C(x_1^2 - x_2^2)/D^*,$$

where h'_1 and h'_2 are values of the slope $h'(x)$ at x_1 and x_2 , respectively. Finally, $h'_2 = \infty$ occurs at some value of x_2 , where

$$x_2 = x_0 \leq [x_1^2 + D^*/C(h'_1)^2]^{1/2}.$$

This proves the contention, since the expression on the right is a finite upper bound on x_0 .